Estimating Human Movement Using a Three Axis Accelerometer

A Qualifying Examination Presented in Partial Fulfillment of the Requirements for the Degree Doctor of Philosophy

Eric Cope

Department of Electrical Engineering

Arizona State University

Co-advisors: Prof. Antonia Papandreou-Suppappola

Prof. Bahar Jalali-Farahani

March 9, 2009

Contents

1 Introduction

As the computational power of digital circuitry follows Moore's Law, the ability to process biological waveforms in an advanced manner becomes a reality. What was previously thought impossible, is now possible, not only in doctors' office computers, but also in extremely low power implantable devices. As the computational power is harnessed, the medical device industry will be able to push their diagnostic processing far beyond basic timers and rectifiers to determine R to R wave intervals in Electrocardiograms (ECG) or simple brain alpha wave detection in Electroencephalograms (EEG). Additionally, there have been many technological advances in sensor capabilities far extending the basic electrical field sensing capabilities of yesterday. Such advanced sensors range from pH sensors detecting stomach acid strength to potassium sensors measuring cellular diffusion processes and accelerometers measuring human motion, respiration, and heart sounds.

The combination of these new sensor modalities and new processing power is enabling new disease diagnosis, disease management and improvement, and objective quality of life metrics. These improvements benefit both doctors and patients. They benefit patients because doctors diagnose their diseases sooner and more effectively as well as manage the disease as it is treated. Additionally, doctors benefit because they can treat patients quicker, easier, and more reliably, keeping patients out of their office and home taking advantage of their improved quality of life.

The goal of this research is to study methods of using three-axis accelerometers to detect, classify, and trend human motion. Once this information is determined, several aforementioned benefits can be realized including measuring the change in quality of life and detecting cardiac and neurological diseases. Examples of disease detection and further explanation of quality of life metrics are discussed later in this report.

There has been significant research in the area of human motion analysis. This research can typically be divided into two types. The first type of research is usually performed by people with a biological or physiological background. The biological analysis is typically very

deep and complex, however the engineering, specifically the signal processing, is very shallow and simple. The other type research is performed by engineers with a deep understanding of the signal processing requirements and methods, but the biological applications are high level and have little application. For instance, there are simple ECG processing algorithms that incorporate basic low pass filtering. On the other hand, there are very advanced processing algorithms requiring time-frequency analysis to detect simple R-waves. The void between these types of research is where actual applications of advanced processing techniques lies and where we classify this research.

In this manuscript, we consider the application of three-axis accelerometers for estimating the motion parameters of cardiac patients, following the work of [1]. This application has not been studied in detail, and very few publications can be found on it. Using a simple state formulation, we estimate human motion parameters using a Kalman filter. Another important point of this research is implementation. Depending on the final algorithm selection, we plan to implement the algorithm in digital hardware that can meet the standards of an implantable device. This puts substantial limits on the types of mathematical operations that can be performed in order to detect and classify different types of human motion. These limits are typically constrained on data throughput limited by clock speed and power consumption. This manuscript is organized as follows. In Section 2, we first discuss the physiology of human motion and the different ways of sensing that motion as it pertains to this research. In Section 3, we discuss the research we did on current algorithms and implementations of human motion estimation. In Section 4, we discuss the work we did to implement the Kalman filter. Finally, Section 5 is the conclusion and discussion of future work.

2 Physiology of Human Movement

The physiology of human movement is a very complex system with many business drivers in the biomedical world. If a system were designed that could classify and trend human movement, many types of applications would improve. For instance, the quality of life of a patient is often subjectively determined through an interview process with the patient. This interview is dependent on factors outside its scope and is therefore influenced. For example, if the medication the patient is taking causes severe undesired drowsiness, the patient may lie regarding their perceived health in order to be taken off their medication. If the physiology of human movement could be accurately classified and trended, the quality of life for that patient could be determined and trended. For instance, if the patient spends all day lying down with little movement, they are typically in bed suffering from pain, weakness, or other limiting factors. However, if the amount of time spent in bed developed a trend downward, then the doctor could safely assume the patient is more actively participating in life. This trend becomes an objective metric for measuring quality of life.

There are additional applications in human movement classification and trending. Certain diseases have physiologic signatures that can be detected by analyzing human movement. For instance, there exists a cardiac disease that causes severe chest pain if the patient sleeps on a particular side. However, if a patient rolls over to their other side, the pain goes away. So what does the patient do? Typically, they assume it is indigestion or gas and roll over and fall asleep. In order for a doctor to discover this disease, an in-depth patient interview must be conducted focusing on this type of disease. However, if a device, external or implantable, could detect this type of human movement (sleeping on a particular side), then the diagnosis of this disease would be far easier.

By providing health practitioners with this type of information, many improvements can be made for the patient. That is the ultimate goal of all biomedical research: improve proper diagnosis rates while reducing diagnosis time; reduce time spent in medical care facilities like hospitals and doctors' offices; improve the patient's quality of life; and a system that can

classify and trend physiological human movement

2.1 Human Movement

The basis of this research is classifying human movement. Human movement can be classified as four major classes of movement; lying down, sitting, standing, and walking/running. These states are depicted in Figure 1.

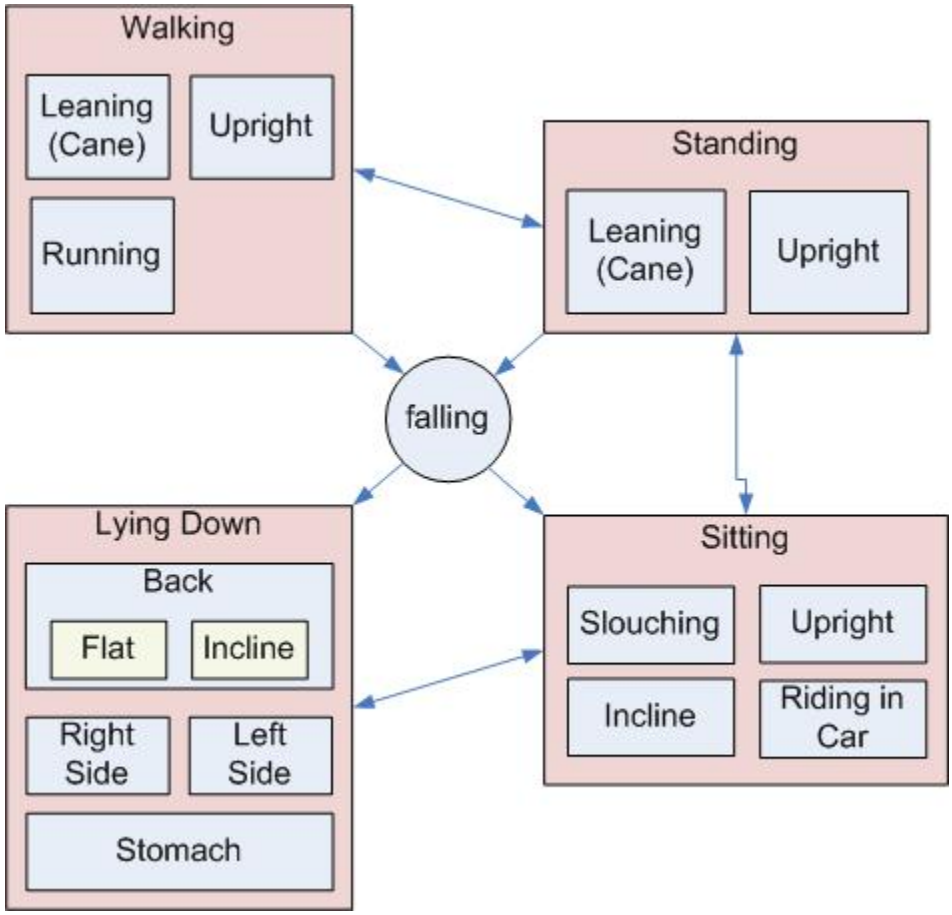

Figure 1: States of Human Movement

There are subclasses within each class defining further each class. For instance, when the person is lying down, they could be lying on their back, side, or chest. Knowing how the person is lying can be very important for diagnosis. Also note that each class is not completely defined. This is not a complete list of all subclasses because each disease or treatment may need a custom signature. This research aims at addressing the most common types of

human movement with extrapolation to more specific movement signatures as dictated by the doctor. Each type of motion deserves its own discussion below.

The most broadly applied human movement state is lying down. This state is used in more diagnoses and metrics of quality of life than any other motion (or lack of motion). If a patient is spending all day in bed, then it is fair to assume that that patient is suffering and their quality of life is severely impaired. There are five common subclasses within the class of lying down. A patient may lie down on their back, their stomach or chest, their left side or their right side. Additionally, a patient may lie on their back at an incline. It is very typical for a heart failure patient to lie on an incline. Heart failure patients suffer from an accumulation of fluid in their lungs. It is common for a heart failure patient to die of suffocation due to fluid in their lungs before their heart finally quits. Patients lie on an incline to allow them to breathe until doctors can prescribe the appropriate drug cocktail customized to their chemistry and condition. If a patient is able to sleep at less of an incline, this can be indicative of reduced fluid in their lungs, indicating an effective drug regimen. This information provided to a doctor is a very powerful tool for improving their patient's lives.

Sitting is another major human movement state. This is an important state for two reasons. First, it provides an intermediate state in between lying down and standing. Second, it is the most common conscious state. We sit at our desks at work. We sit while watching television. We sit while reading books and magazines. We sit in cars, trains, and airplanes. Knowing how much a person is sitting, or more precisely, how much more or less a person is sitting, can be indicative of the quality of life. If a patient is sitting more, possibly slouching, instead of tending their garden or walking around the neighborhood, this will inform their doctor that a change in therapy is necessary.

Standing is another important state of human motion. It is also a transitory state between sitting and walking/running. If a patient is able to transition from using a cane to walking on their own, this is an obvious symptom of a successful hip replacement. However, if that

replacement bothers them at certain times of the day, this can indicate sensitive inflammation in an area that needs to be addressed. Also, some patients fall while standing due to a number of reasons, not limited to syncope (the patient's heart stops for a period of time causing loss of consciousness), seizures, and fatigue. If suddenly the patient transitions from a standing state to a lying down state, it is possible the patient fell. If a patient fell, then an implantable device may need to deliver a therapy. The detection of the fall helps reduce false detections of disease, another important benefit to the patient.

The final major state is walking or running. A healthy patient will be able to participate in walking and running activities. If a patient is walking less due to a mis-prescribed drug cocktail, a doctor can catch this sooner to remedy the situation. Finally, a transition from walking to lying down is also a case for falling, possibly detrimental to the patient, but equally vital to know so as to deliver the appropriate therapy.

2.2 Types of Sensors

There are several types of electro-mechanical sensors that can determine the state of human movement. Each sensor has its benefits and deficits. The features important to the application of this research include power consumption, size, processing requirements, implantability, mechanical reliability, cost, and manufacturability. Each of these features will be discussed below as necessary.

2.2.1 Accelerometers

Accelerometers are sensors that measure acceleration experienced by their bodies. A simplified drawing of an single axis accelerometer sensor is in Figure 2. The simple accelerometer has springs on two opposite sides of a mass. When the accelerometer substrate moves, the mass will remain in place until the springs apply a force, pulling the mass in the direction of the substrate. As those springs compress and expand, parasitic capacitors intentionally built into those springs change values. These values are measured and used to determine the

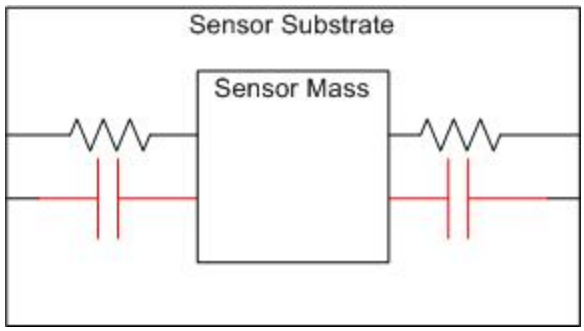

Figure 2: A simplified single axis accelerometer

amount of force the mass is experiencing due to the springs. Using Newton's law, $F = m * A$, where m is the mass and A is the acceleration, one can calculate the acceleration the sensor is experiencing. For example, a simple calibration test often conducted on accelerometers is to align the sensor's sensitive axis with that of gravity. Gravity is easily measured by an external source as well as the sensor. By trimming the sensor, we can calibrate it to a known DC value.

There are two major types of accelerometers. The first type is described above and most often realized using Micro-Electrical-Mechanical Systems (MEMS) technology on a silicon substrate. This type of sensor is cheap compared to other sensors, easy to manufacture in high volumes due to established wafer processing techniques, and is capable of low power applications. Another type of sensor is based on piezo electronics. Piezo electronics produce a voltage based on vibrating the molecular structure. This type of sensor cannot sense DC type signals such as gravity which prevents its use in the applications of this research. Any further reference to accelerometers in this paper will be to the MEMS based sensor. Several pictures of packaged MEMS devices are seen in Figures 3, 4, 5.

2.2.2 Gyrometers

Gyroscopes are another type of sensor that senses angular momentum. It typically has a spinning wheel or mass. When the sensor is rotated, the spinning rate is affected as well as the direction of spin in Cartesian coordinates. The power requirements are far too high to

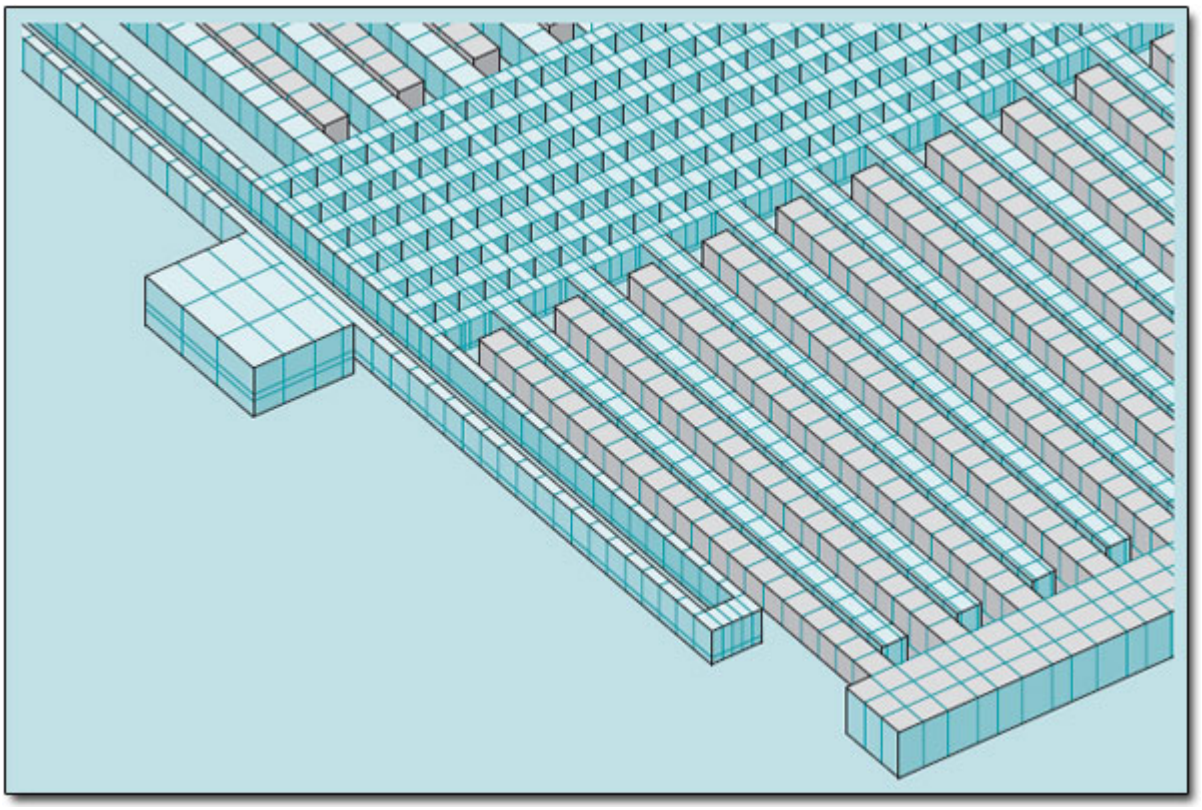

Figure 3: A MEMS Accelerometer Finger Structure: Courtesy of Sandia National Labs

use gyroscopes in an implantable system. An illustration of a basic gyroscope is in Figure 6.

2.2.3 External Sources

There are several external devices which can detect human movement. One method is to use a camera system that uses image processing to determine the states of the person and then process further those states. Sonar can be used similarly to determine human movement. However, both methods require a fixed point to mount the camera or sonar device which limits its use to clinical settings which is not feasible for implantable devices.

2.3 Types of Measured Acceleration

Because accelerometers are the most feasible sensor for use in implantable devices, they will be the focus of the rest of the research. When measuring acceleration in human movement,

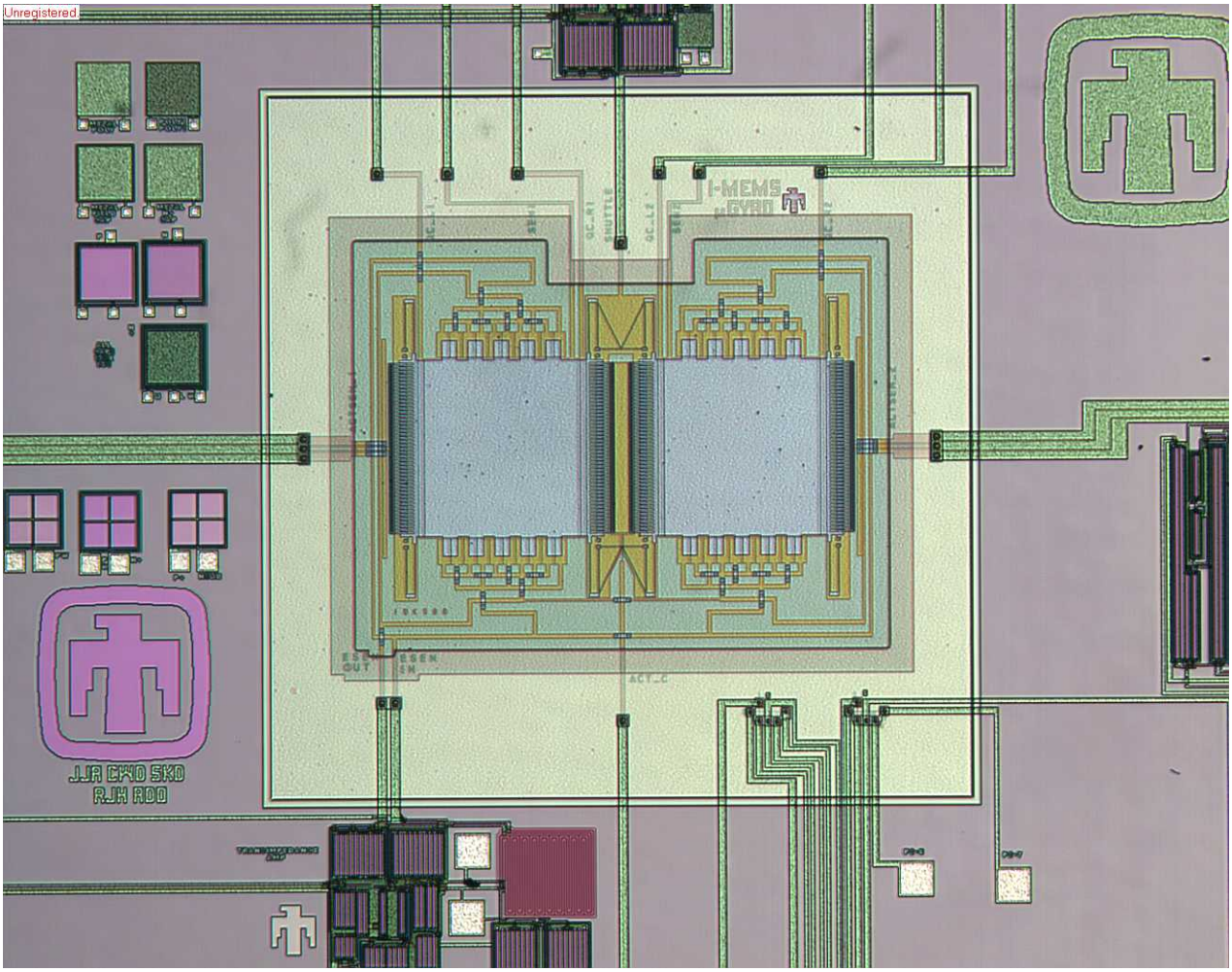

Figure 4: A MEMS Accelerometer Die Photo: Courtesy of Sandia National Labs

we must first understand the underlying physical principles of acceleration and the types before we try to measure, process, and detect the different states of human movement. The basic equation of acceleration, $a(t)$ is the second derivative of position, $x(t)$ with respect to time

$$a(t) = \frac{d^2x(t)}{dt^2} \tag{1}$$

There are two forms of acceleration, linear and angular acceleration. Both are important when measuring human movement. Of these types of acceleration, there are two causes for acceleration. The first and most important is gravity. The second and most interesting is human movement causing accelerations. All four points will be discussed next.

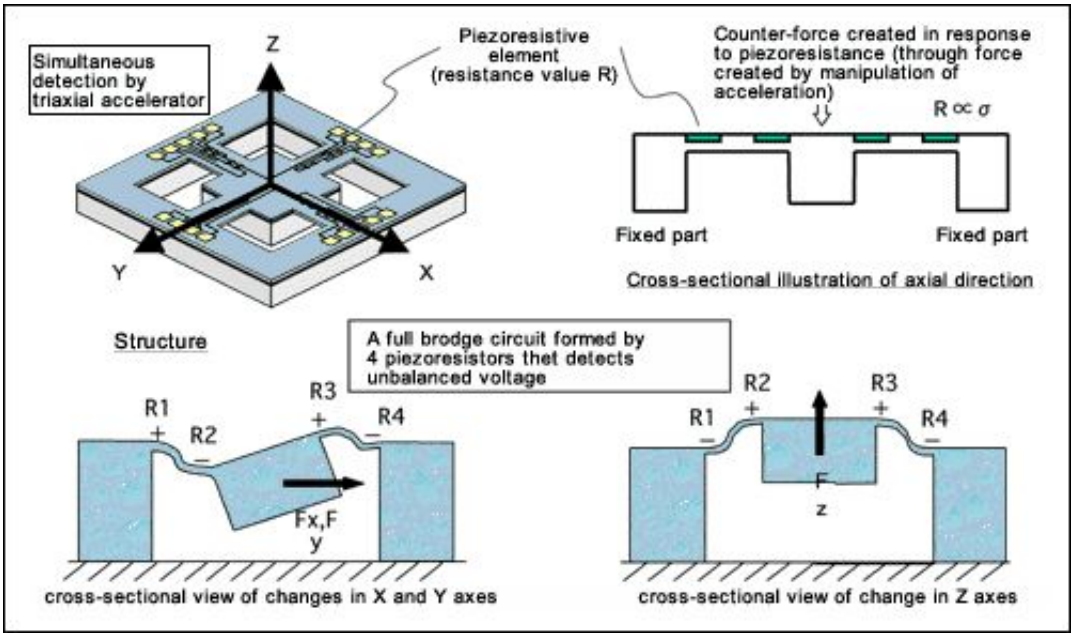

Figure 5: A MEMS Accelerometer Illustration: Courtesy of Hitachi

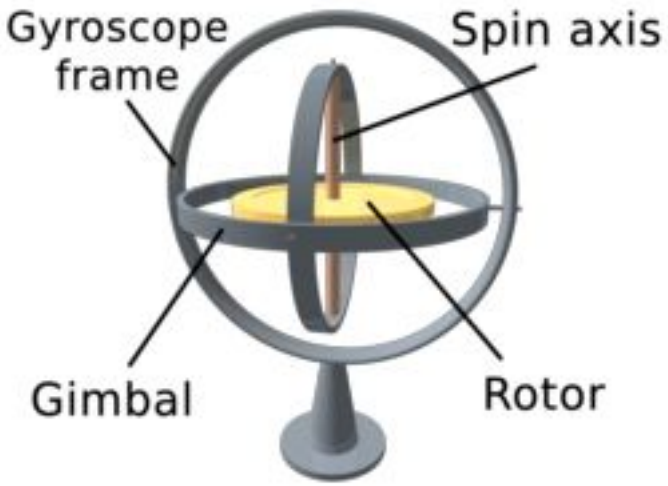

Figure 6: A Gyroscope Illustration: Courtesy of Wikipedia

2.3.1 Linear Acceleration

Linear movement is movement along a straight line. Linear acceleration is the acceleration experienced during this type of movement. A simple example of linear acceleration is that of a rock dropped. It falls straight down and experiences a linear acceleration in the -z direction. This is the easiest type of acceleration to detect. It does not require special accelerometers

to detect any direction of acceleration. Position can be simply calculated by integrating acceleration twice. It is the primary type of acceleration humans experience during walking, standing, sitting, and lying down, typically due to gravity. However, once angular movement is introduced, the problem of separating human motion accelerations from gravity increases dramatically.

2.3.2 Angular Movement

Angular acceleration is acceleration around a point in space. It is typically specified in radians (or degrees) per second squared (rad/s^2). A human can experience angular acceleration if they bend over (the sensor is typically implanted in the chest which pivots around the hips) or spin around a point. This is a difficult acceleration to measure and can require a specific type of accelerometer. Depending on the length of angular acceleration, it can look like a DC acceleration (like gravity) or like linear acceleration such as when bending over.

2.3.3 Gravity

The most constant and most useful form of acceleration is gravity. Gravity is always pointing down towards the center of the Earth. It is fairly constant, assuming the person's distance from the center of the Earth is constant. For purposes of this research, the gravitational unit is g where 1 g = 9.8 m/s^2. Since we are researching in a three dimensional space (x, y, z), the gravity vector is defined as (0,0,-1) in units of g. The unit g is often used to describe accelerations in relation to the gravity experienced on Earth. It is the direction in which a pendulum points when no longer moving. The gravity never moves in the absolute frame of reference. It can move as quickly as a human can move their torso in the sensor frame of reference. Frames of reference will be discussed later in this report.

2.4 Signals of the Accelerometer

When using an accelerometer to measure human movement, it is imperative to understand the signals embedded in the accelerometer measurement. There are four main types of signals. Gravity is the main signal, always found in the accelerometer signal. Human movement will always exist even when the patient is not moving due to things like breathing and rocking. The third signal is offset which will be described below. The final signal is noise.

2.4.1 Gravity

Gravity is the largest signal we will measure. Generally other signals will be discussed in terms of gravity (the motion experienced had a magnitude of 1 g). It is used to calibrate the system during manufacturing as well as recalibrate the system's alignment once implanted. Most papers written rely on gravity being the largest signal of the accelerometer in order to do further processing. It is treated as the baseline. Once gravity is detected, processing is assumed completed, so this is the most important signal to measure.

2.4.2 Movement

The accelerations experienced during human movement are the real pieces of information sought after in this research. Differentiating between walking and standing requires the ability to detect that human movement. Detecting the difference between falling and sitting down requires the ability to process properly human movement. Human movement is made up of both linear accelerations and angular accelerations, making it very difficult to properly identify movement signatures.

2.4.3 Offset

There are several different types of offsets that the sensor will experience during its lifetime. The sensor will not remain calibrated due to a number of reasons. The first reason is mechanical wear. Because MEMS accelerometers rely on a mechanical mass moving left and

right, and up and down, there will be wear on the springs and the mass. An important part of manufacturing the sensor is reducing the impact of sensor wear. Another important type of offset is possible. Some accelerometers use mutual beams. That means that some beams, or blocks of mass as described in Figure 2, are used during calculations of accelerations in the x and y direction. Most sensors measure how much charge is necessary to charge those parasitic capacitors. If charge is left over from a previous measurement, then this can cause an offset. This offset is signal dependent making it very hard to model and detect. Again, this kind of offset is sensor-dependent.

2.4.4 Noise

The final signal in the accelerometer measured data is noise. There are several types of noise in accelerometer signals, usually grouped together as "noise". The first is electrical noise found in the semiconductor systems measuring the capacitance and digitizing that signal. The second type of noise is the vibrations the sensor experiences including sound (voice, music, etc.) and breathing. These types of signals may have applications like heart sound detection, but are beyond the scope of this research project. Usually, this noise is modeled as white Gaussian for simplifying analysis, yet this is not always the case.

2.5 Frames of Reference

Because acceleration is a vector, it needs to be referenced to a specific coordinate frame. The coordinate frame specifies the directions of the x, y, and z vectors in Cartesian coordinates. There are two coordinate frames important to this research. The first coordinate frame is the Global Coordinate frame. That always has the negative z vector pointing toward the center of the earth. The second coordinate frame important to this research is the physiological coordinate frame. This frame always aligns with the test subjects body. The negative z axis is always pointing down the body towards the feet. The y axis stretches laterally across the chest with the y vector pointing towards each shoulder. The x axis points out from the chest

with the negative x axis pointing out of the back of the subject.

3 Use of Accelerometer Sensors

In this chapter, we discuss previous research in the area of three axis accelerometer (3AA) signal processing and their applications.

3.1 A MEMS based MicroSystem for Monitoring Frail Activity

The authors in [2] describe two kinds of sensors used to detect daily activity of individuals, typically frail elderly patients. The authors use both accelerometers and magnetometers to detect and qualify activities such as walking and sitting. Their research was focused on determining the optimum number of sensors and their locations as well as the optimum sampling frequency. They also focused on detecting transitions between physical states. They found that a single sensor cluster, one three axis accelerometer and a magnetometer, placed on the chest was the optimum place for their application. They also found that a sampling rate of 30Hz was more than adequate to properly sample their signals.

The processing of the sensor data included calculating the three angular orientations (rolling, pitching, and lacing). Then they used a median filter followed by a low pass filter to select only the low frequencies of the movements of interests. They classified the angle of the torso in five classes. These classes determined if the person was standing straight up, lying down on their stomach, lying down on their back, or transitioning between these three states. Their conclusion was that by using both the three axis accelerometer and the magnetometer, they could easily detect the states important to determining the quality of life of their patients.

3.2 Estimating Energy Expenditure using Triaxial Accelerometers

The authors in [3] were interested in measuring energy expenditure during fitness sessions of athletes. They were concerned with energy expenditure during the activities of walking, running, sprinting, and stationary movement (standing). The authors conducted two studies

using treadmills. The triaxial accelerometer system was attached via an elastic belt around the waist. The sensor was sampled at 24 Hz. A 0.9 Hz Rectangular Window Finite Impulse Response filter was used to separate out the orientation (gravity) and the human motion component. Then, the integral was taken for 10 second intervals of the human motion component to estimate the energy expenditure.

3.3 Articulated Human Motion Tracking Using Tri-Axis Sensors

The authors in [4] were also interested in analyzing human motion, however they did it with a multi-sensor package. That included a tri-axis accelerometer, a tri-axis magnetometer, and a tri-axis gyroscope. They performed some preliminary research that demonstrated that current methods for using only a tri-axis accelerometer was insufficient for their applications. Additionally, they created a 15-segment humanoid model to accurately identify the best location to place their sensor package. The authors also noted a limitation of magnetometers. These sensors are extremely sensitive to local magnets and other ferrous materials. Their recommendation was to keep these materials away from the sensors, which is impractical for our application. The authors intended to have 15 sensor units placed on each segment of the patient. Additionally, they proposed to use a Kalman filter with an update frequency of 20 Hz as the method of orientation estimation. Their experimental results showed good estimation using the Kalman filter. However, the Kalman filter had a time lag of approximately one second, which is too long for out application.

3.4 Microaccelerometer for Target Classification

The authors in [5] used accelerometers and Artificial Neural Networks (ANN) to track vehicle targets. Their method was to measure seismic signals of moving targets and recognize these waveforms using ANN. This paper as a demonstration of advanced methods of processing accelerometer data. The authors sampled at 4 kHz, which is dramatically higher than our application. Even though their application was drastically different than our application,

their method may be applicable, however more research in this area is needed.

3.5 Adaptive Noise Cancellation With Accelerometers

The authors in [6] used two adaptive filtering techniques, Least Mean Squares (LMS) and Recursive Least Squares (RLS), to determine the motion of a human patient to filter out ECG artifacts directly related to the motion. There is a lower bound where the motion stops corrupting the ECG signal, therefore not requiring adaptive filtering. However, during periods of high activity, the degree of corruption is significant, requiring the adaptive filtering mentioned. The authors used a single axis accelerometer with a bandwidth of 0.11 - 20 Hz, and used a sampling rate of 500 Hz, limited by their digitizer board, not by the sensor data. While the adaptive filtering took place on the ECG waveforms, this paper demonstrates yet another reason for determining and classifying human motion.

3.6 Detection of Knee Unlock Using Accelerometry

The authors in [7] wanted to detect when a knee was locked or unlocked. Their application was for rehabilitating paraplegics. They used accelerometers to detect a specific human body motion, the knee locking. To focus on that area, they placed two single axis accelerometers on the leg of the patient. They were sampled the data at 100 Hz and anti-alias filtered the data at 35 Hz. No advanced filtering was needed to obtain the data necessary for their application. The authors low pass filtered the data and counted thresholds to determine whether the knee was unlocked or locked.

3.7 Functional Activity Monitoring

The authors in [8] consider an application similar to the one we are concentrating on. They want to detect and classify human movement to assist rehabilitating individuals with motor disorders. The authors used a hybrid sensor using an accelerometer and an electromyographic

(EMG) probe, which studies electrical impulses and their control of muscle activity. The authors wanted to study the same four principal activities that we want to study; sit, stand, walk, and lie. The authors focused on artificial intelligence methods such as Time-Dependent Neural Networks, Blackboard and rule-based technologies. There was no mention of sampling rates or types of sensors used (i.e. tri-axis accelerometers).

3.8 Accelerometers for Gesture Awareness

In [9], the use of accelerometers for detection of gestures, similar to the Nintendo Wiimotes, was described. This paper also had a power limit with regard to the degree of processing allowed on the accelerometer waveforms. This paper does not have the power limit requirements we need for our application, however, the authors discuss some decisions based on power constraints. For instance, they used a first order Butterworth low pass filter to filter the accelerometer data instead of a more advanced filter due to power constraints. They also used thresholding and comparing instead of an advanced filter to detect motion, a very common approach in embedded devices.

3.9 Linking Gait Characteristics With Waist Accelerations

In [10], the goals for processing human movement are similar to our objectives. The authors discuss using the Discrete Cosine Transform as a means of feature extraction, and they used this transform to detect harmonics of the gait cycle. They placed the accelerometer on the waist of the patient, instead of the chest in our application. Then, using Levinson-Durbin recursion, they generated a linear predictive model to derive the harmonic frequencies. Although a very promising method, there are few too many computations for an embedded system.

3.10 Measurement of Joint Angles Using Accelerometers and Gyroscopes

Accelerometers and gyroscopes were used in [11] to measure the angles of leg joints. They used four accelerometers and four gyroscopes to measure and calculate the angle of the knee. Their processing consisted of a low pass filter and some physics-based modeling. All signals were sampled at 200 Hz. They also used a Savitzky-Golay smoothing filter as a post-processing step to smooth the data. They also noted that skin motion artifacts were a strong source of error in their experiments. They used a low pass filter to address the artifacts.

3.11 Monitoring Human Posture and Walking Velocity Using Accelerometers and Gyroscope

The authors in [12] sought to monitor human posture and walking velocity using accelerometers and gyroscopes. They used three accelerometers, one attached to chest, thigh, and knee. Additionally, a gyroscope was attached to the knee. All four sensors were sampled at 60 Hz. The accelerometers were low pass filtered at 3 Hz. The gyroscope was band pass filtered between 0.3 and 20 Hz. This particular sensor network allowed the authors to detect human posture within their limit of error.

3.12 Human Motion Analysis Using a Kinematic Sensor

The authors in [13] used two accelerometers and a single piezoelectric gyroscope to analyze human motion. They sampled at 40 Hz and low pass filtered the data at 17 Hz. They post processed their data using Discrete Wavelet Transforms (DWT). They first did a DWT of vertical acceleration using a third order Daubechies mother wavelet. Then, depending on the results of the first wavelet, they would perform another wavelet using the Coiflet order five mother wavelet. They also explained several assumptions for classifying human motion. For

example, if two contradictory states were detected (i.e. walking and sitting), then preference was given in this order: lying down, walking, standing to sitting transition, and sitting to standing transition. Another example was that if a patient was detected to be leaning back, they decided to rotate the frame of reference because their patients were very unlikely to be leaning backwards (typically, elderly people lean forward, to lean on a cane for example).

3.13 Measurements of Heart Motion Using Accelerometers

The topic in [14] is slightly different from the rest of the work discussed thus far. This author researched the use of accelerometers to measure heart motion during surgery. In order to use a rhythm detection system to detect rhythms (the heart beat) and detect any changes to that rhythm. The authors used a three axis accelerometer and sampled the accelerometer 250 Hz, however the bandwidth of the sensors was under 50 Hz.

3.14 Measurement of Human Movement Using a 3-D Accelerometer

The work in [1] provides a good foundation for our future research. The authors used a single accelerometer to detect human movement and a Kalman filter to process the data to detect the different states of human movement. They placed the sensor on the back of their patients. They sampled at 100 Hz. One interesting point is that these authors were the only ones to mention the mass of the sensing unit. Since this unit acts as a low pass filter and attenuator to movement, this is a very important piece of information. They were able to achieve an error of 2 degrees root mean square (RMS) for their functional three dimensional test movements. This was twice as accurate as simply low pass filtering the accelerometer data. This paper will be discussed in more detail later.

3.15 Location and Sensitivity Comparison of MEMS Accelerometers

The authors in [15] used eigenvector analysis to analyze multiple single axis accelerometers and a single three axis accelerometer. They sampled at 256 Hz and low pass filtered at 50 Hz using a fourth order filter with 0.1 dB of pass band ripple and 50 dB of stop band attenuation.

3.16 Identifying Gait Pattern with Accelerometers

The authors in [16] wanted to identify individuals based on the pattern of their movements. They specifically wanted to use walking patterns to identify users of cell phones and other portable electronics. They sampled at 256 Hz and compared the fast Fourier Transform (FFT), histograms, and higher order moments as methods for classifying the user of their device.

3.17 Orientation Estimation with Gyroscopes and Accelerometers

The authors in [17] briefly discusses the use of a Kalman filter to estimate human body orientation using three single axis accelerometers and a gyroscope. The Kalman filter was used to estimate the tilt by fusing accelerometer data and gyroscopic data.

3.18 Human Posture and Walking Speed Using Accelerometers and Gyroscope

The authors in [18] used three two-axis accelerometers attach to the back, the thigh, and the shank. The sensors were sampled at 60 Hz. The accelerometers were low pass filtered at 3 Hz and the gyroscopes were band pass filtered between 0.3 and 20 Hz.

3.19 Bluetooth Module for Fall Detection

The authors in [19] use an accelerometer, a tilt sensor, and a gyroscope to detect falling in human patients. Their algorithm was very light on the required signal processing. It was more of a finite state machine with thresholding of sensor data. There was no mention of sampling rate. A part of our research was determining the minimum sample rate necessary to determine human motion. By reducing the sampling rate, we can reduce the power consumption of our embedded system.

3.20 Physical Activity and Behavior Map Monitoring

The authors in [20] developed a system to map human behavior into a monitoring system. They used a piezo-resistive accelerometer. The accelerometer data was low pass filtered at 0.1 Hz in order to detect walking and running. There was no mention of sample rate.

3.21 Activity Sensors for Rate-Responsive Pacemakers

The authors [21] in compares activity sensors used in pacemakers. This is the final target of our research. Rate-Responsive pacing is defined as using activity sensors (typically accelerometers) to detect activity in the patient to increase or decrease the pacing rate, much like normal hearts increase their rate during periods of activity. This paper sampled at 256 Hz and used a threshold detector to count pulses in activity. This paper demonstrates the shear lack of innovative in medical devices and their accelerometer processing and shows the need to extract more information from raw accelerometer data to improve the patient's quality of life.

3.22 Position and Orientation Tracking Fusing Magnetic and Inertial Sensing

The authors in [22] use magnetic sensors and accelerometers to track human position and orientation. The authors use a Kalman filter to process the data. They use the magnetic sensor to provide a long term stable assessment of relative positions.

3.23 Telemetry System of Daily Life Motion and Arrhythmia

The authors in [23] describe a system to measure electrocardiograms (ECG) and accelerometer data. The accelerometer data is sampled at 50 Hz. The authors found that a filter was necessary to properly detect the motion they were seeking.

3.24 Energy Expenditure Using Triaxial Accelerometers

The authors in [24] used accelerometers to measure energy usage in athletes. The sensors were mounted on the L4-L5 medial lumbar vertebra region of the test subject. They used two two-axis accelerometers to create a tri-axial sensor. They were sampled at 150 Hz. They low pass filtered the data at 0.9 Hz using a Hamming windowed Finite Impulse Response (FIR) filter.

3.25 Accelerometers Analysis

The authors in [25] was to allow athletic performance to be analyzed using accelerometers. They used triaxial accelerometers sampled at 250 Hz per channel. The authors specific application was swimming performances. The data was low pass filtered. An important note here is the higher sample rate used to capture and discriminate between different high level activities. If we could lump together all high level activities, the sampling rate may be reduced.

3.26 Accelerometry-Based Movement Classification

The authors in [26] wanted to detect three postures; sitting, standing, and lying. Two biaxial accelerometers were used to build a three axis sensor mounted to the waist of the test subject. The sampling rate was 45 Hz. The authors used Shifted Delta Coefficients to calculate the body acceleration components. This method required fewer computations than a FFT based method. The back end classification was performed using a 32-mixture Gaussian Mixture Model. A separate Gaussian Mixture Model was trained for each movement type using the Expectation Maximization algorithm.

3.27 Gait Assessment by Accelerometry

The authors in [27] used six single axis accelerometers as two triaxial accelerometers to assess gait of humans. The sampling rate was 128 Hz. The authors used a 2048 order FIR filter. The 3dB points are set around the basal frequency of the walking. There is no mention of where the sensors were attached, however the authors imply around the knee.

3.28 Human Movement Classifier Using a Triaxial Accelerometer

The authors in [28] used a single triaxial accelerometer attached to the hip of a test subject to classify movement. The same basic postures mentioned above are classified. The sensor had a bandwidth of 100 Hz. The sensor was sampled at 45 Hz. The authors suffered several constraints that we will also suffer. First, there is no knowledge of future events. Second, the amount of data that can be buffered is limited (the author was limited to 1 second, we may be allowed more). The amount of processing time available was limited (due to the real-time application). The first filter in their processing flow was a median filter. the second step was a low pass third order elliptical filter with a cut-off frequency of 0.25 Hz. This was employed to separate gravity from body-related accelerations. This paper was especially important because of the constraints placed on the authors regarding processing power, data storage,

and sensor bandwidth.

4 Kalman Filter Based Estimation of Human Motion

We follow the work of Luinge and Veltink [1] to study three axis accelerometer processing and human motion. This paper uses the Kalman filter to estimate the inclination of a human torso using sensor measurements. We will first describe the Kalman filter and present the algorithm in [1]. We will then consider an alternative human motion estimation algorithm.

4.1 The Kalman Filter Models

The Kalman filter is a method to estimate unknown states given measurements [29]. For the Kalman filter to yield the optimal estimate, there are several assumptions that must be met. The first assumption is that the observed noise and the process modeling any errors in the state space model must be additive Gaussian processes. Additionally, you must be able to model the system using linear equations. However, most systems do not meet these assumptions exactly. Some systems can be linearized so that an extended Kalman filter can still provide good estimation performance. If the system is highly nonlinear, then sequential Monte Carlo methods, like particle filtering, need to be used [29] [30].

In order to use the Kalman filter, the system state and measurement equations need to be available. For a system with unknown state variable, $\mathbf{x}_k$, at time k, the state equation is given by

$$\mathbf{x}_k = F_k \mathbf{x}_{k-1} + \mathbf{w}_k \tag{2}$$

that relates the current state to the previous state. F_k is the state transition model. It describes how the state transitions from time $k-1$ to time k. $\mathbf{w}_k$ is the modeling error process noise with covariance Q_k. Since the true state of the system is impossible to measure, we must use the observation equation to relate the measurement $\mathbf{z}_k$ to the state $\mathbf{x}_k$, i.e.,

$$\mathbf{z}_k = H_k \mathbf{x}_k + \mathbf{v}_k \tag{3}$$

where H_k is the observation model that relates the state to the observation, and v_k is the observation noise with covariance R_k. Note that, without accurate models or accurate statistical information on the noise, the estimated state will not be optimal.

4.2 Predict and Update

The Kalman filter can be described using two equations, the prediction and the update. The first step is to predict the future state using

$$\hat{\mathbf{x}}_{k|k-1} = F_k \hat{\mathbf{x}}_{k-1|k-1} \tag{4}$$

$\hat{x}_{k|k-1}$ is the predicted state at time k given information from time $k-1$, and $\hat{\mathbf{x}}_{k-1|k-1}$ is the state estimate at time $k-1$. The predict equation is the predicted estimate covariance,

$$P_{k|k-1} = F_k P_{k-1|k-1} {F_k}^T + Q_{k-1} \tag{5}$$

where T denotes transpose, $P_{k|k-1}$ is the predicted estimate covariance at time k using information from time $k-1$, $P_{k-1|k-1}$ is the updated estimate covariance at time $k-1$ using information from time $k-1$, and Q_{k-1} is the process noise covariance at time $k-1$.

After computing these values, the next step is to compute the update equations. The first step is to compute the innovation, sometimes referred to as the measurement residual

$$\tilde{\mathbf{y}}_k = \mathbf{z}_k - H_k \hat{\mathbf{x}}_{k|k-1} \tag{6}$$

Next, the innovation covariance, S_k, is calculated as

$$S_k = H_k P_{k|k-1} {H_k}^T + R_k \tag{7}$$

The Kalman gain is given by

$$K_k = P_{k|k-1} {H_k}^T {S_k}^{-1} \tag{8}$$

Next, we must calculate the updated state estimate

$$\hat{\mathbf{x}}_{k|k} = \hat{\mathbf{x}}_{k|k-1} + K_k \tilde{\mathbf{y}}_k \tag{9}$$

The final equation provides the updated estimate covariance, $P_{k|k}$

$$P_{k|k} = (I - K_k H_k) P_{k|k-1} \tag{10}$$

where I is the identity matrix. Using these equations, one can estimate the state of a system by looping recursively through these equations. Next, we will discuss how the authors in [1] applied these equations to process three axis accelerometer data and extract human torso inclination.

4.3 The Model

The three axis accelerometer measurement is modeled as [1]

$$\mathbf{z}_k = \mathbf{a}_k - \mathbf{g}_k - \mathbf{b}_k + \mathbf{v}_{A,k} \tag{11}$$

where $\mathbf{z}_k$ is the sensor output at time k, $\mathbf{a}_k$ corresponds to the accelerations due to linear and rotational movement, $\mathbf{b}_k$ is the offset of the sensor, and $\mathbf{v}_{A,k}$ is the observed noise. Note that these variables are vectors, pointing to a direction in a three dimensional Cartesian coordinate system

$$\mathbf{z}_k = \begin{bmatrix} z_k^x \\ z_k^y \\ z_k^z \end{bmatrix} \tag{12}$$

. The second component, $\mathbf{g}_k$, is the gravity component. The $\mathbf{b}_k$ term describes any offset introduced to the sensor. For example, most accelerometers of interest to the medical industry today are MEMS based mechanical sensors. As such, they suffer the same mechanical problems its larger counterparts experience including wear and tear, fatigue, and mechanical stress. As a part wears, the sensor output experiences an offset, described here by

$$\mathbf{b}_k = \mathbf{b}_{k-1} + \alpha \tag{13}$$

where α is some modeled constant. Note that in [1], no specific state equation as in (2) was provided.

The authors in [1] make several assumptions regarding this problem statement. The first assumption is that the accelerations, $\mathbf{a}_k$, must be zero mean. Even a tiny offset from the zero mean would result in extremely large displacements just a few seconds into the model due to the nonlinear relationship between acceleration and distance in (1). The second assumption is the bandwidth of the human body's possible accelerations. The acceleration experienced by the human body is limited due to the inertial mass, as it behaves like a low pass filter in the mechanical sense. The third assumption is that both the model noise and the observation noise are additive white Gaussian processes. The authors model the human motion acceleration as an autoregressive (AR) process to produce a bandpass response. Also, instead of using the Kalman filter to estimate the acceleration and gravity components, they used the Kalman filter to estimate the errors in the acceleration and gravity components. Their reasoning for this switch was not disclosed.

4.4 Alternative Formulation

Several attempts were made to implement and verify the results in [1], including contacting the authors. However, we discovered that their equations were not complete and not enough information was provided to completely reproduce their results. As a result, we decided

instead to proceed by applying a Kalman filter to the gravity component only. We started by first assuming that the acceleration term and the offset are part of the measurement noise, in order to reduce the dimensionality of the unknown state. Thus, the unknown state in (2) is given by

$$\mathbf{g}_k = \begin{bmatrix} g_k^x \\ g_k^y \\ g_k^z \end{bmatrix} \tag{14}$$

and the measurement equation in (11) simplifies to

$$\mathbf{z}_k = \mathbf{g}_k + \mathbf{u}_k \tag{15}$$

where

$$\mathbf{u}_k = \mathbf{a}_k + \mathbf{b}_k + \mathbf{v}_k \tag{16}$$

is now treated as the observation noise. Note that when

$$H_k = H = \begin{bmatrix} 1 & 0 & 0 \\ 0 & 1 & 0 \\ 0 & 0 & 1 \end{bmatrix} \tag{17}$$

then (3) simplifies to (15). As a part of the future work, we plan to make the observation model more accurate when we also include acceleration in the measurement model.

As part of this research, we developed two state transition models. The first was a simplistic model that uses the linear state transition matrix in (4)

$$F_k = F = \begin{bmatrix} 1 & 0 & 0 \\ 0 & 1 & 0 \\ 0 & 0 & 1 \end{bmatrix} \tag{18}$$

resulting in

$$\begin{bmatrix} x^x_{k|} \\ x^y_{k|} \\ x^z_{k|} \end{bmatrix} = \begin{bmatrix} x^x_{k-1} \\ x^y_{k-1} \\ x^z_{k-1} \end{bmatrix} + \mathbf{w}_k \tag{19}$$

$$\mathbf{x}_{k|k-1} = \mathbf{x}_{k-1|k-1} + \mathbf{w}_k \tag{20}$$

where $\mathbf{w}_k$ is the modeling error process.

In an effort to improve performance without a significant increase in processing, we tried a second model. In the previous model, we claimed that the current sample at time k is, up to some modeling error, equal to the current sample, at time $k-1$, a crude and simple low pass filter. In this version, we assumed that the state at time k depends on the previous two time step state values, at $k-1$ and $k-2$, according to

$$\mathbf{x}_k = 2\mathbf{x}_{k-1} - \mathbf{x}_{k-2} \tag{21}$$

As a result, we now use the state equation in ((2)) but with the state modified to be

$$\begin{bmatrix} x^x_k \\ x^y_k \\ x^z_k \\ x^x_{k-1} \\ x^y_{k-1} \\ x^z_{k-1} \end{bmatrix} = F \begin{bmatrix} x^x_{k-1} \\ x^y_{k-1} \\ x^z_{k-1} \\ x^x_{k-2} \\ x^y_{k-2} \\ x^z_{k-2} \end{bmatrix} + \mathbf{w}_k \tag{22}$$

where $\mathbf{w}_k$ is the modeling error process and the state transition matrix is

$$F = \begin{bmatrix} 2 & 0 & 0 & -1 & 0 & 0 \\ 0 & 2 & 0 & 0 & -1 & 0 \\ 0 & 0 & 2 & 0 & 0 & -1 \\ 1 & 0 & 0 & 0 & 0 & 0 \\ 0 & 1 & 0 & 0 & 0 & 0 \\ 0 & 0 & 1 & 0 & 0 & 0 \end{bmatrix} \tag{23}$$

. Note that the state equation in (22) is greatly simplified from the true nonlinear gravity state equation that we will consider in our future work.

4.5 Simulation Results

As a first attempt towards the motion state estimation, we used the Kalman filter together with one of the state equation models in (19) (Model 1) or (23) (Model 2) and the measurement equation in (15). To generate a testing scenario, we generated a gravity vector of length 4048 samples such that

$$g_k^x = \begin{bmatrix} amplitude \\ \theta \\ \phi \end{bmatrix} = \begin{bmatrix} 1.0 \\ sin(2\pi f_\theta / f_s) \\ sin(2\pi f_\phi / f_s) \end{bmatrix} \tag{24}$$

. Here we used sinusoidal values of θ and ϕ to model oscillating motion in a polar coordinate system. Then, we converted the polar coordinates to cartesian coordinates, as a accelerometer would experience it. For the simulations, we chose a $f_\theta = 0.25$ Hz and $f_\phi = 0.25$ Hz and a sampling frequency of 256 Hz. We used additive white Gaussian noise for the observation noise, assuming known covariance. Using these models, we simulated the system with varying degrees of signal-to-noise ratios (SNRs), ranging from 5 dB to 50 dB for both models.

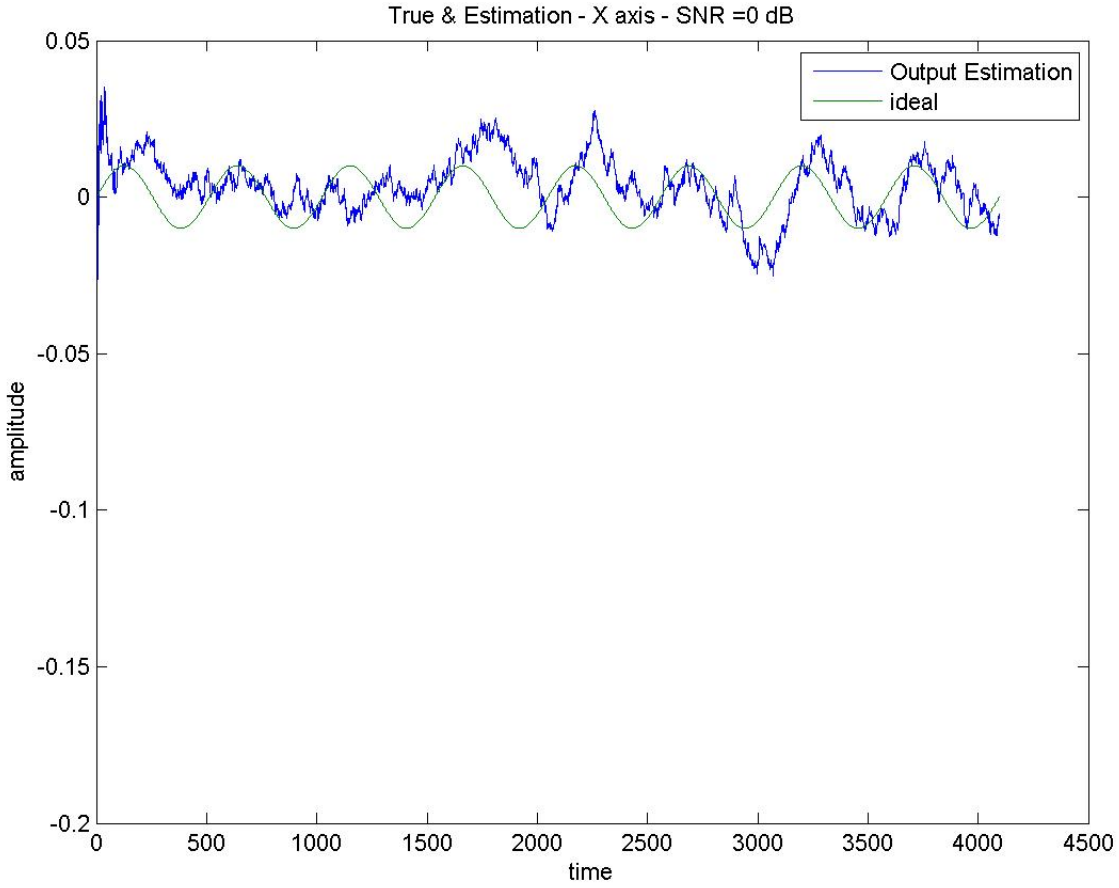

Figure 7: Estimated and true gravity along the x-axis at 0dB SNR for Model 1

The results for Model 1 are shown in Figures 7-21 and for Model 2 in Figures 22-36. For these simulations, I chose a Q of 10^{-6}. To evaluate the impact of choosing Q, I performed Monte Carlo simulations over a range of Q from 10^{-9} to 10^{-4}. Those results are in Figures 37-38.

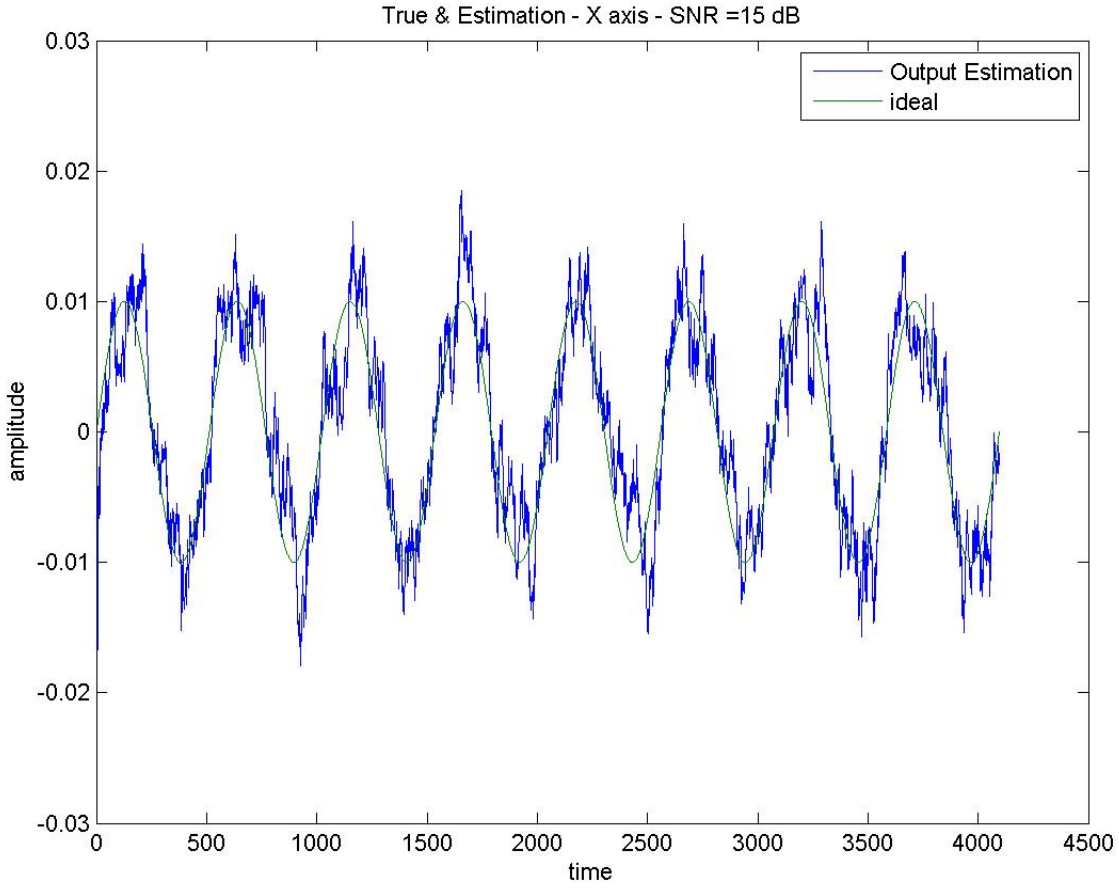

Figure 8: Estimated and true gravity along the x-axis at 15dB SNR for Model 1

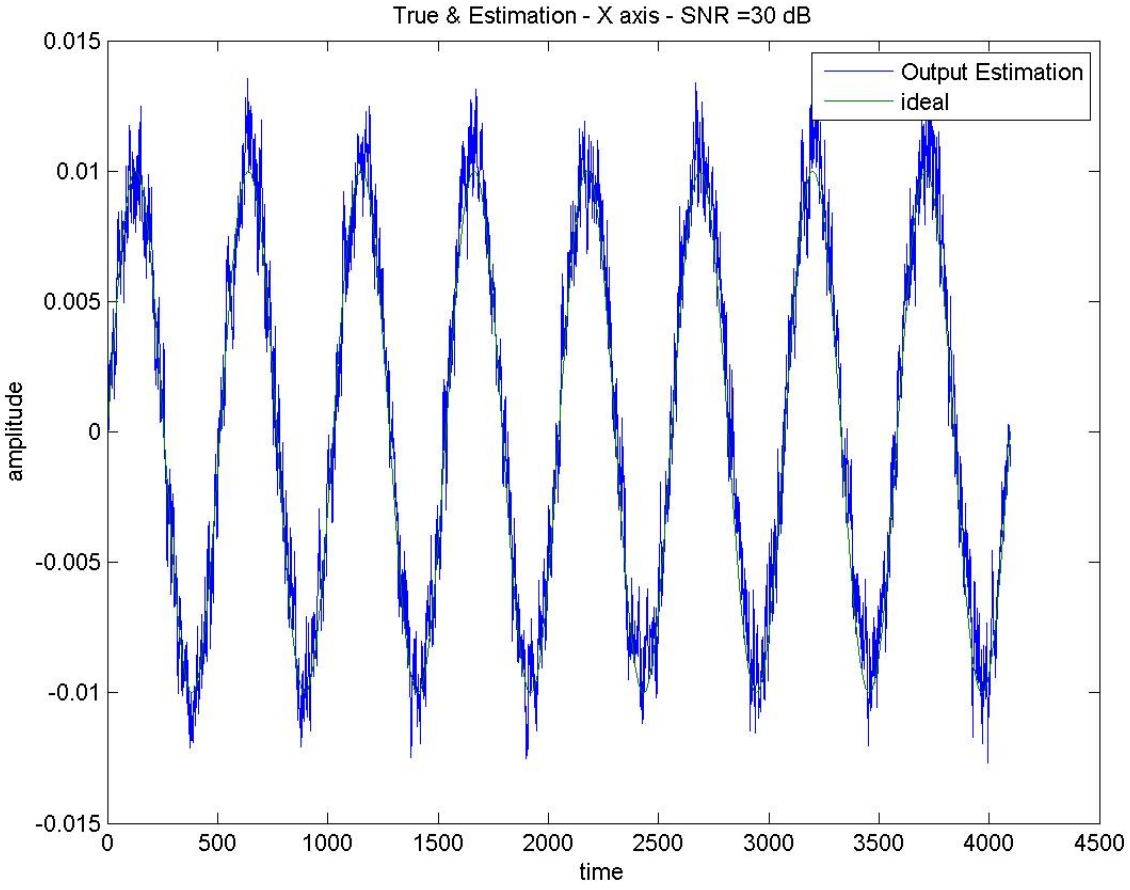

Figure 9: Estimated and true gravity along the x-axis at 30dB SNR for Model 1

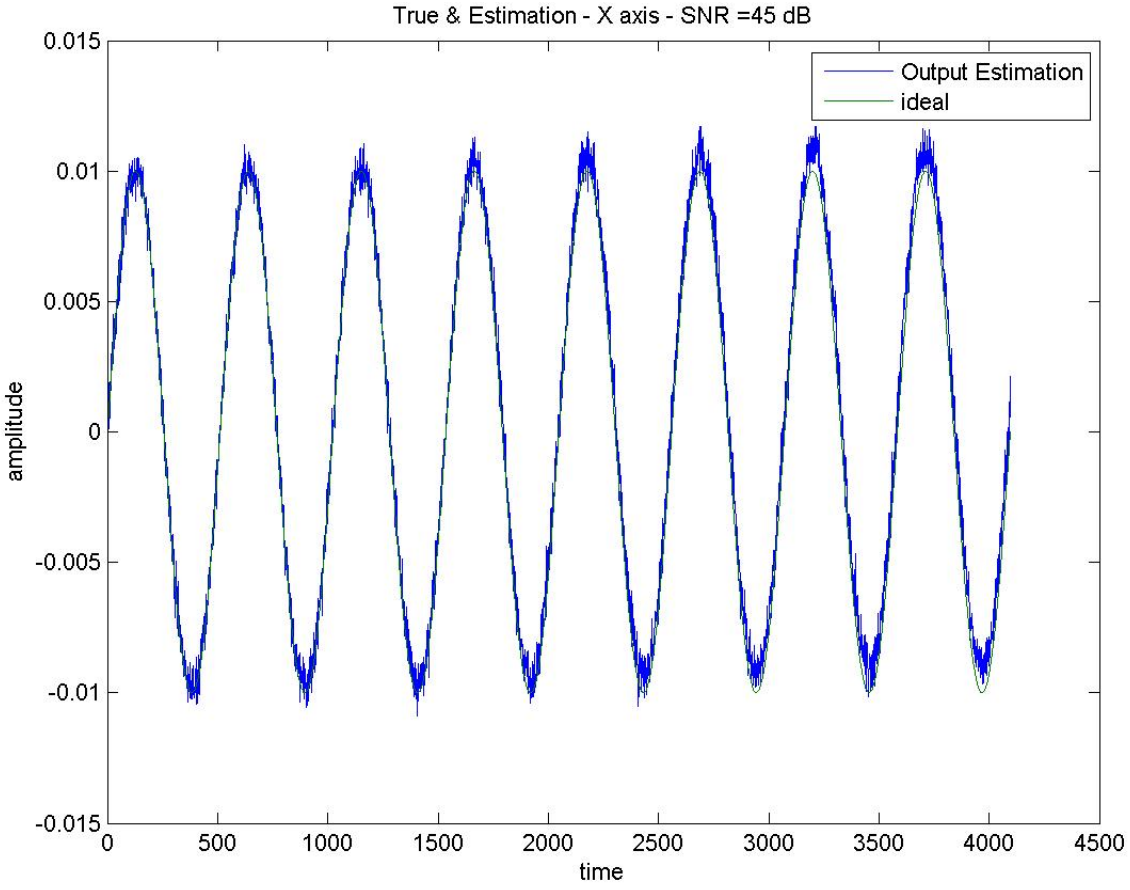

Figure 10: Estimated and true gravity along the x-axis at 45dB SNR for Model 1

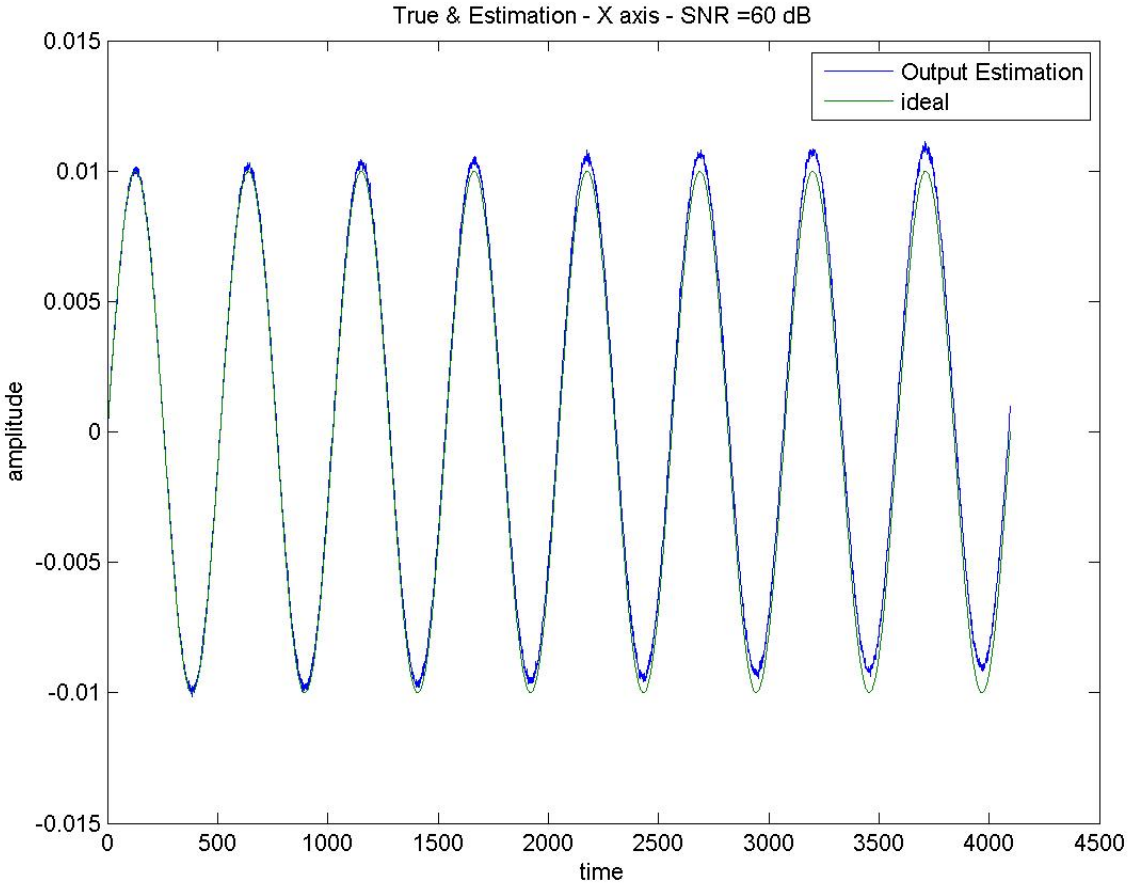

Figure 11: Estimated and true gravity along the x-axis at 60dB SNR for Model 1

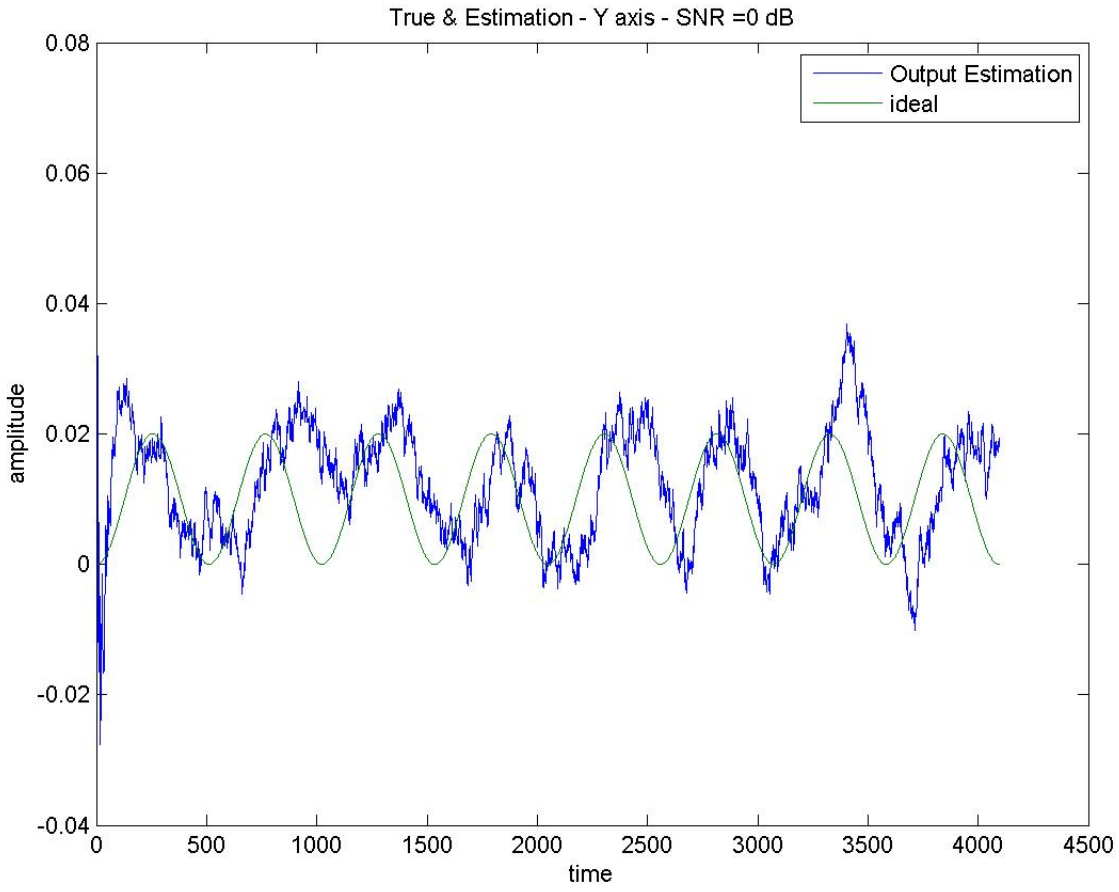

Figure 12: Estimated and true gravity along the y-axis at 0dB SNR for Model 1

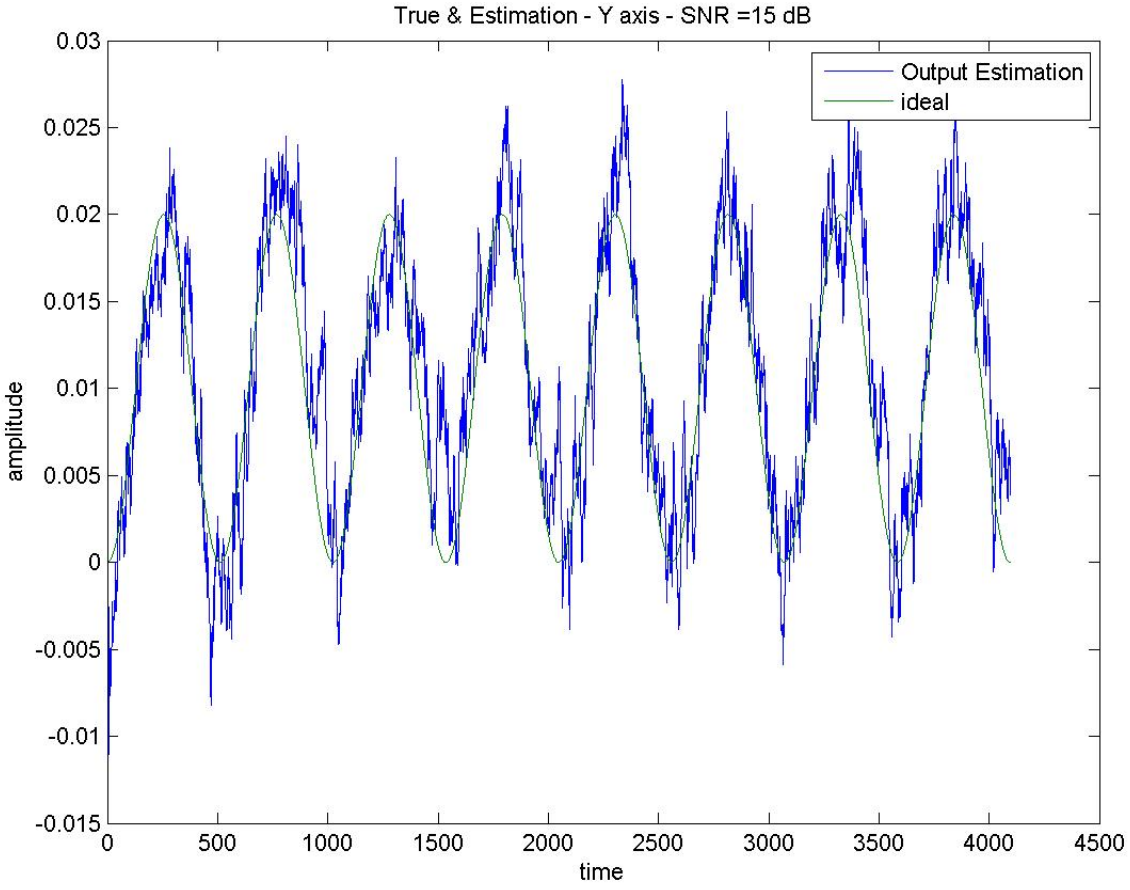

Figure 13: Estimated and true gravity along the y-axis at 15dB SNR for Model 1

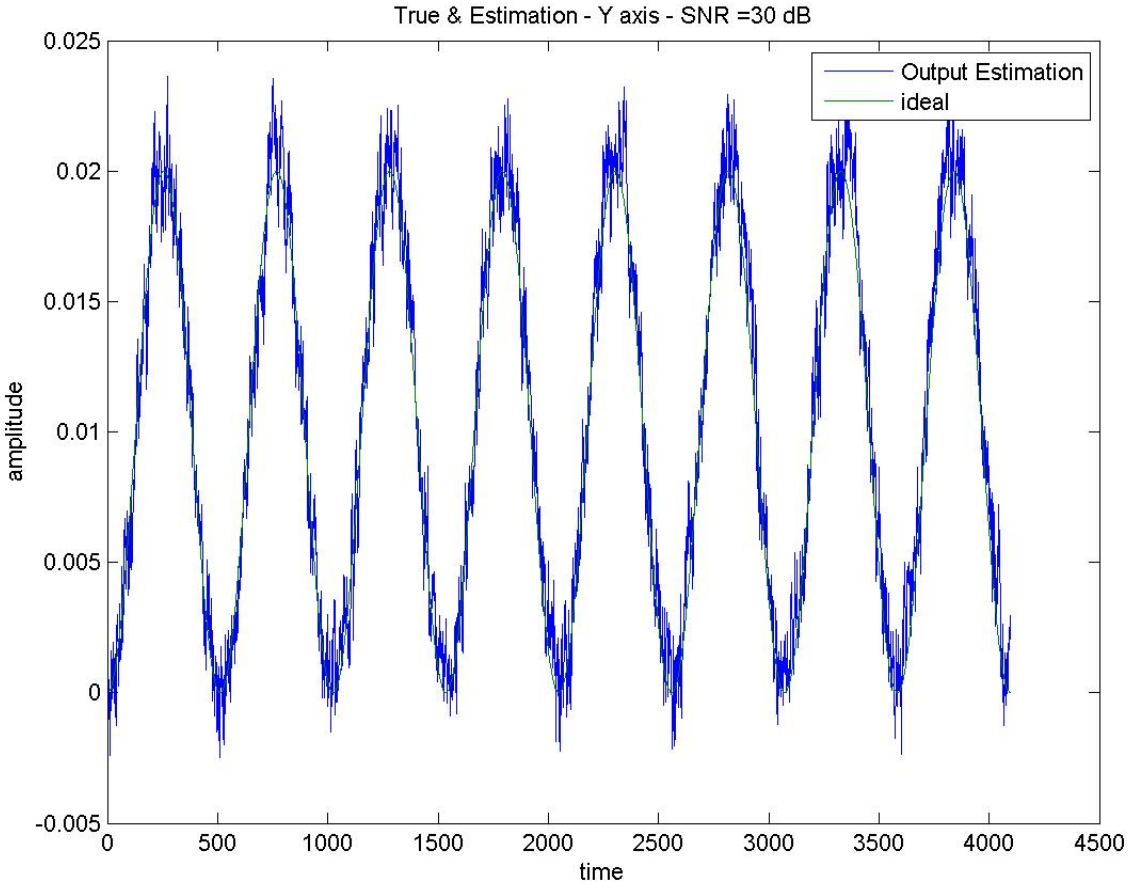

Figure 14: Estimated and true gravity along the y-axis at 30dB SNR for Model 1

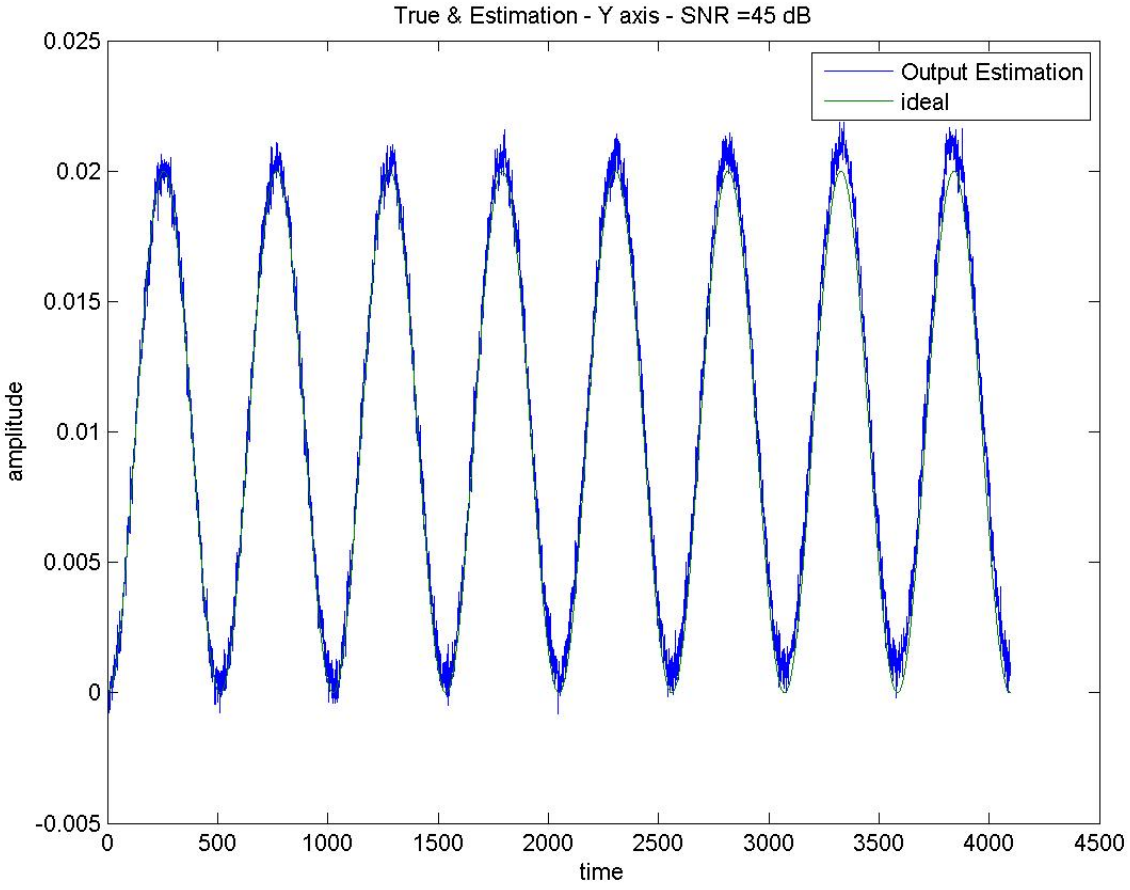

Figure 15: Estimated and true gravity along the y-axis at 45dB SNR for Model 1

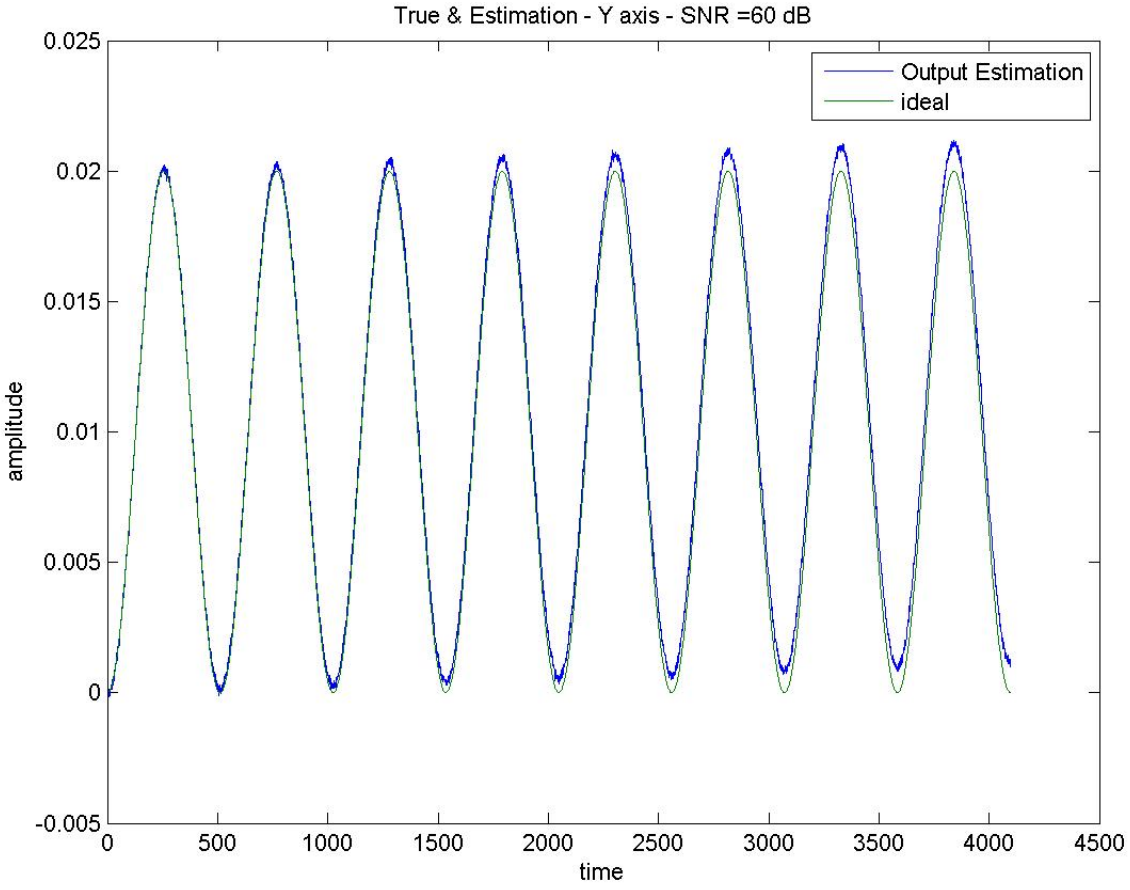

Figure 16: Estimated and true gravity along the y-axis at 60dB SNR for Model 1

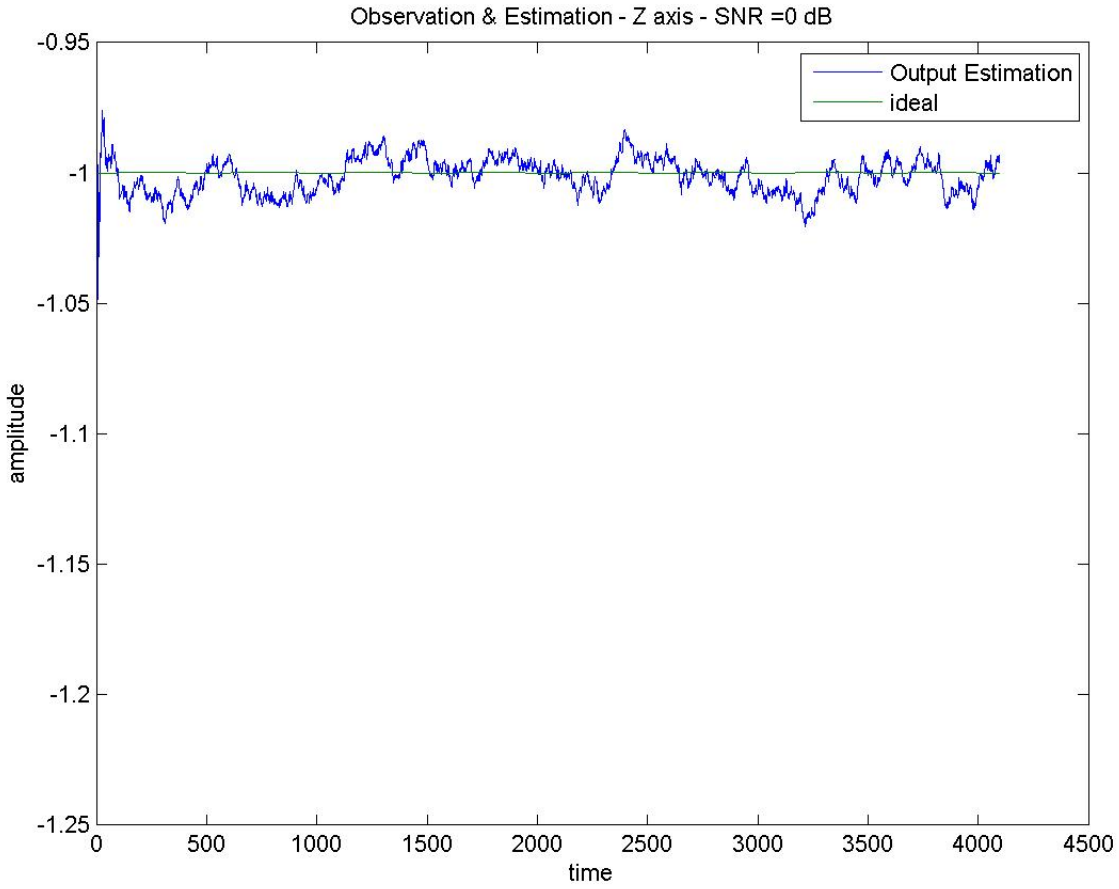

Figure 17: Estimated and true gravity along the z-axis at 0dB SNR for Model 1

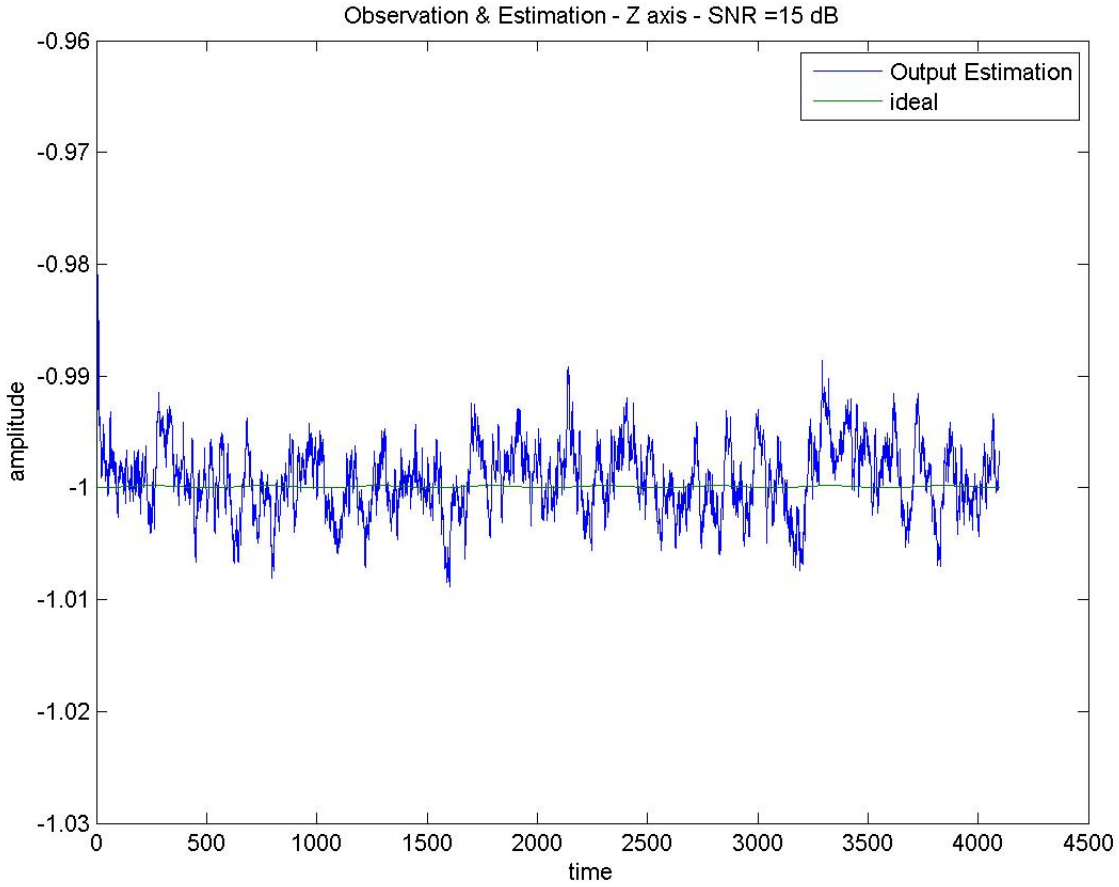

Figure 18: Estimated and true gravity along the z-axis at 15dB SNR for Model 1

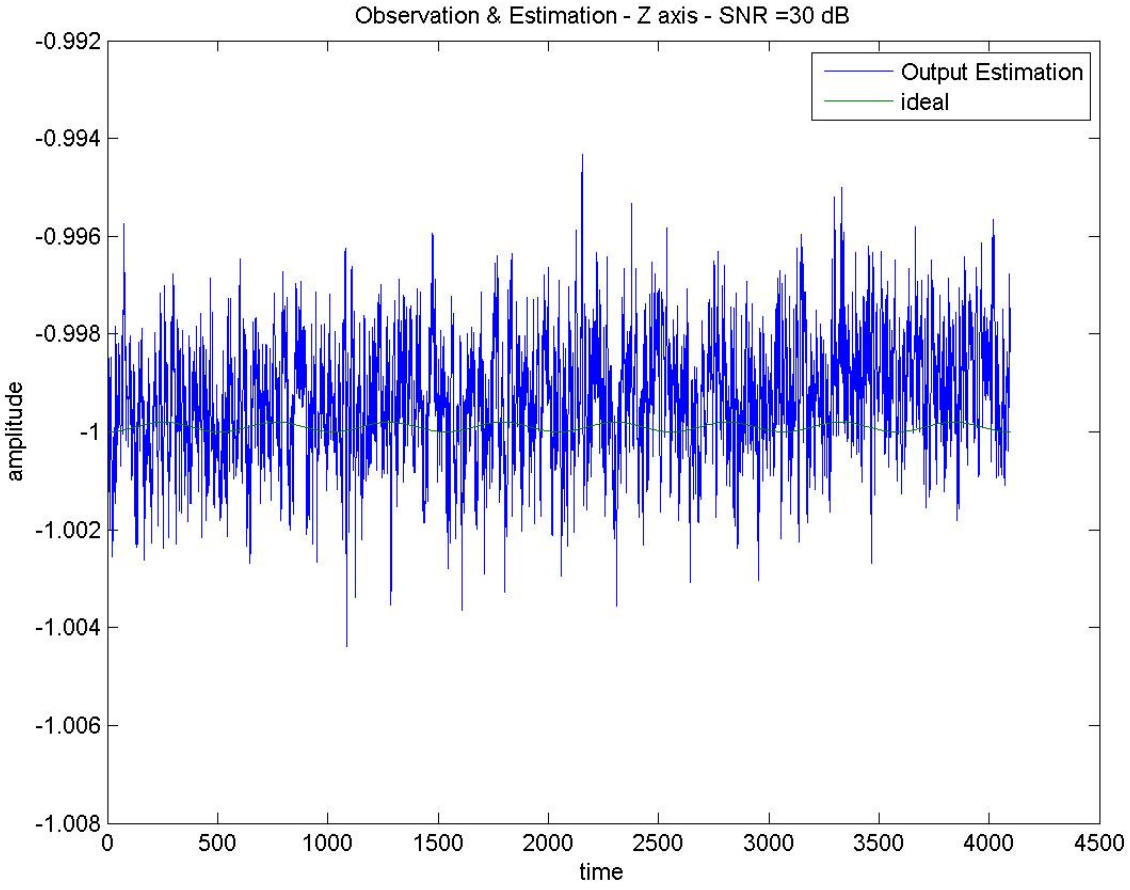

Figure 19: Estimated and true gravity along the z-axis at 30dB SNR for Model 1

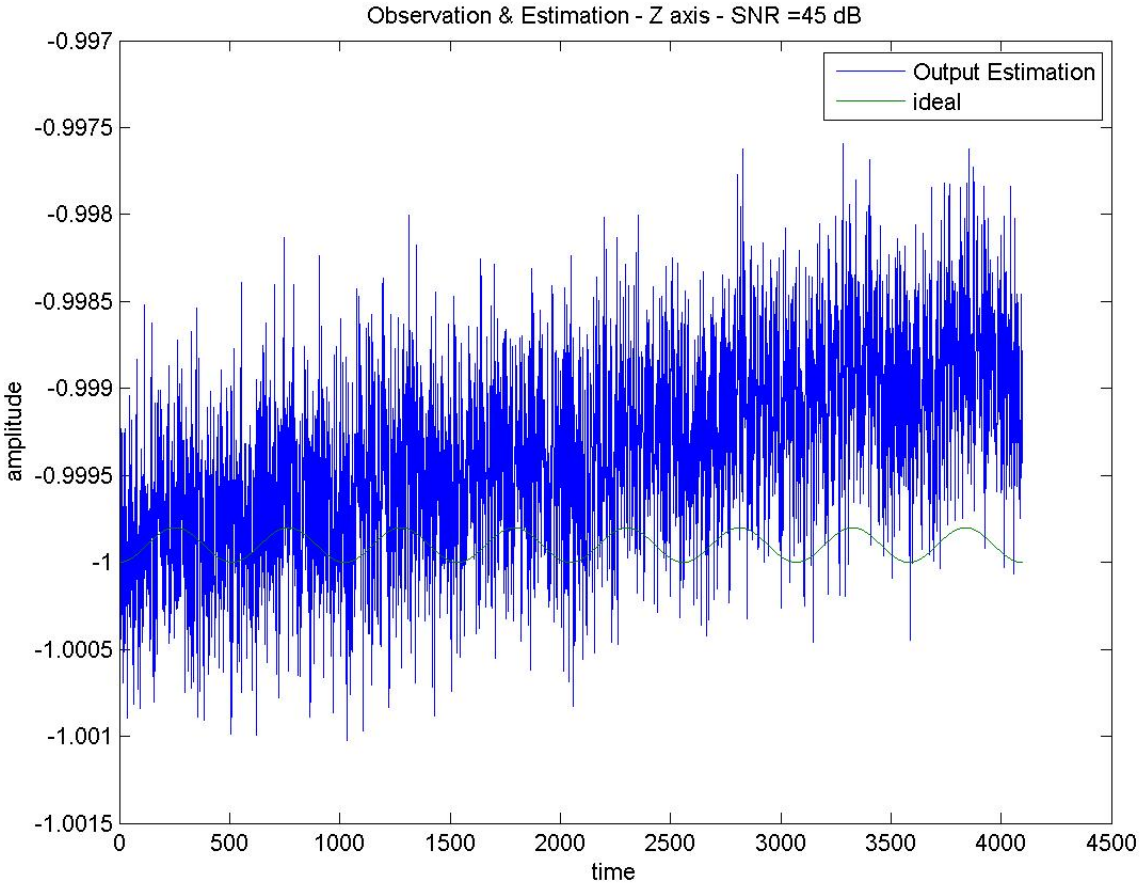

Figure 20: Estimated and true gravity along the z-axis at 45dB SNR for Model 1

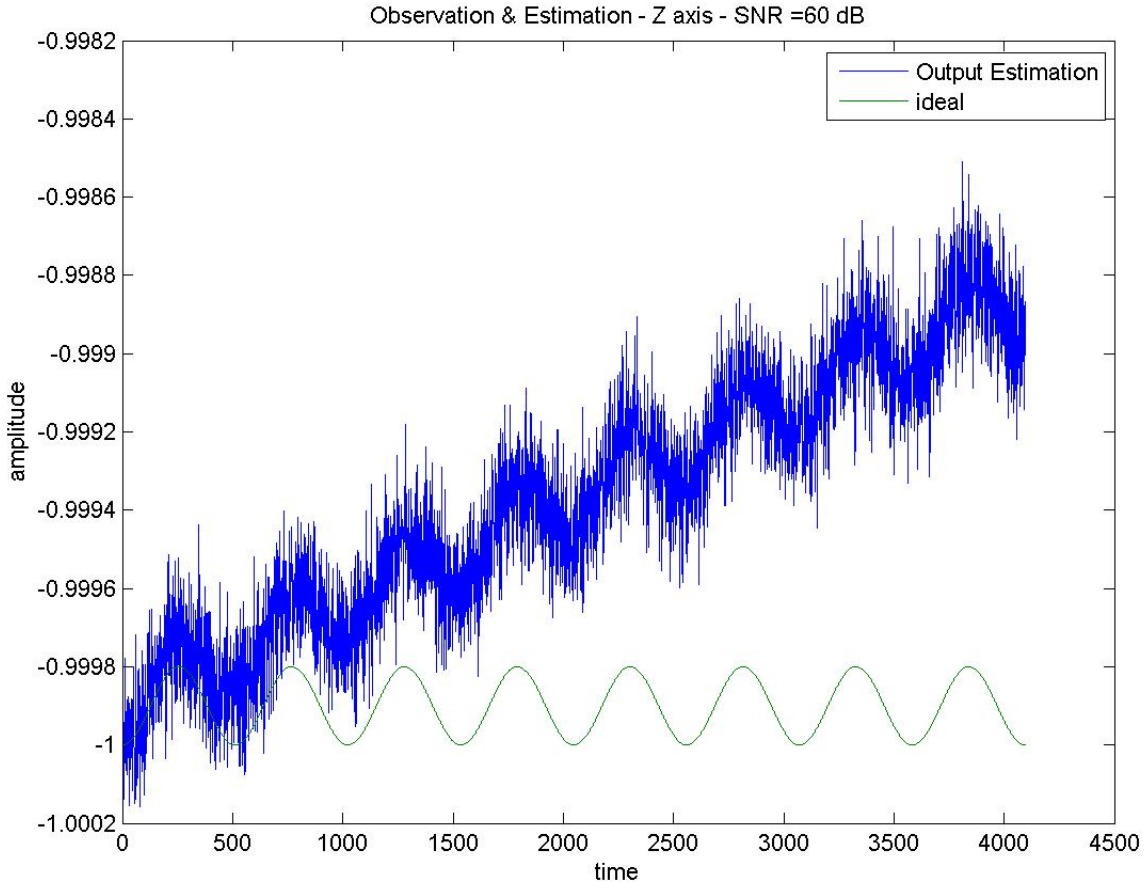

Figure 21: Estimated and true gravity along the z-axis at 60dB SNR for Model 1

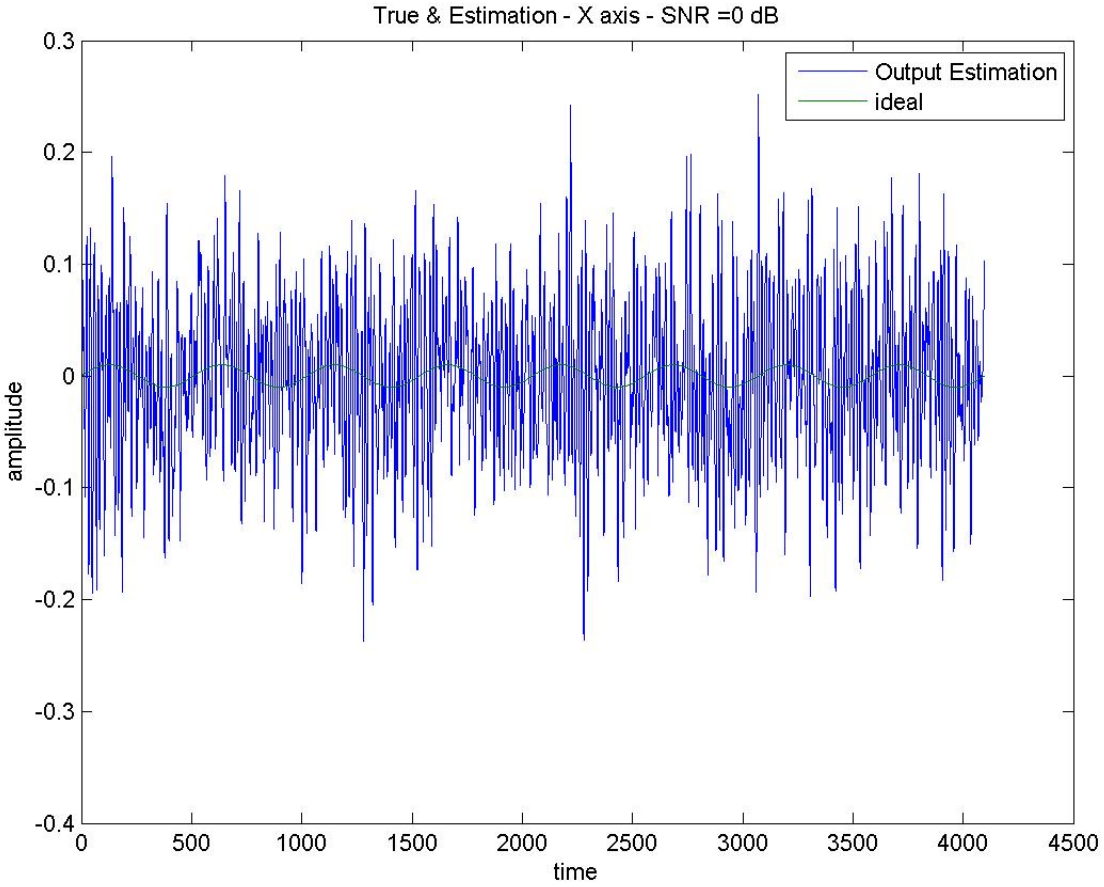

Figure 22: Estimated and true gravity along the z-axis at 0dB SNR for Model 2

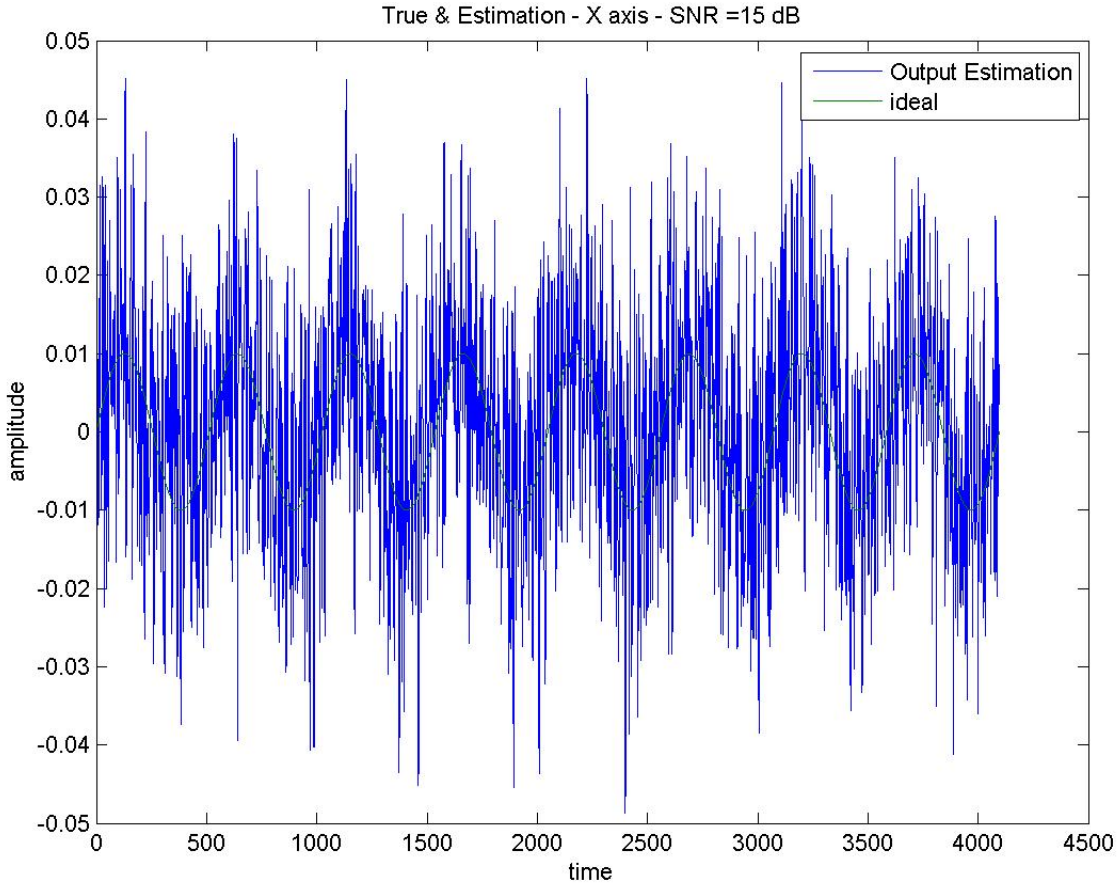

Figure 23: Estimated and true gravity along the z-axis at 15dB SNR for Model 2

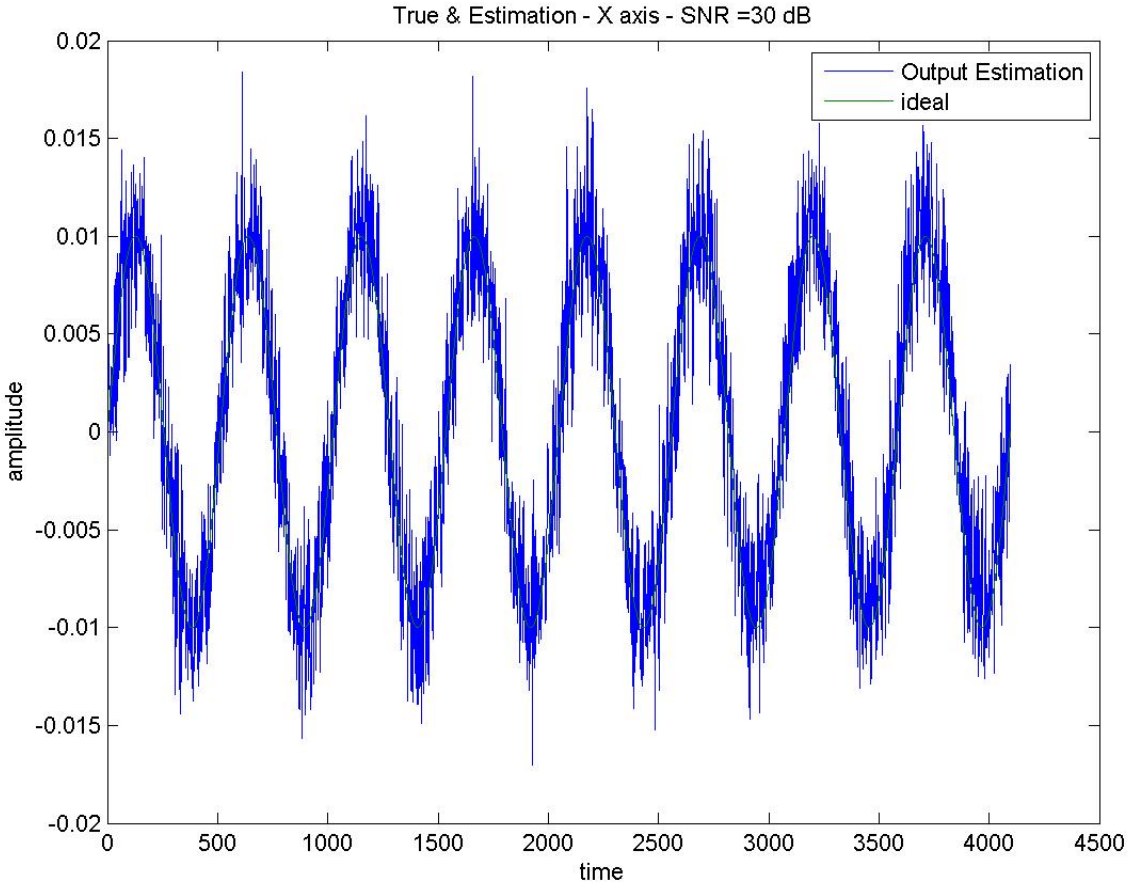

Figure 24: Estimated and true gravity along the z-axis at 30dB SNR for Model 2

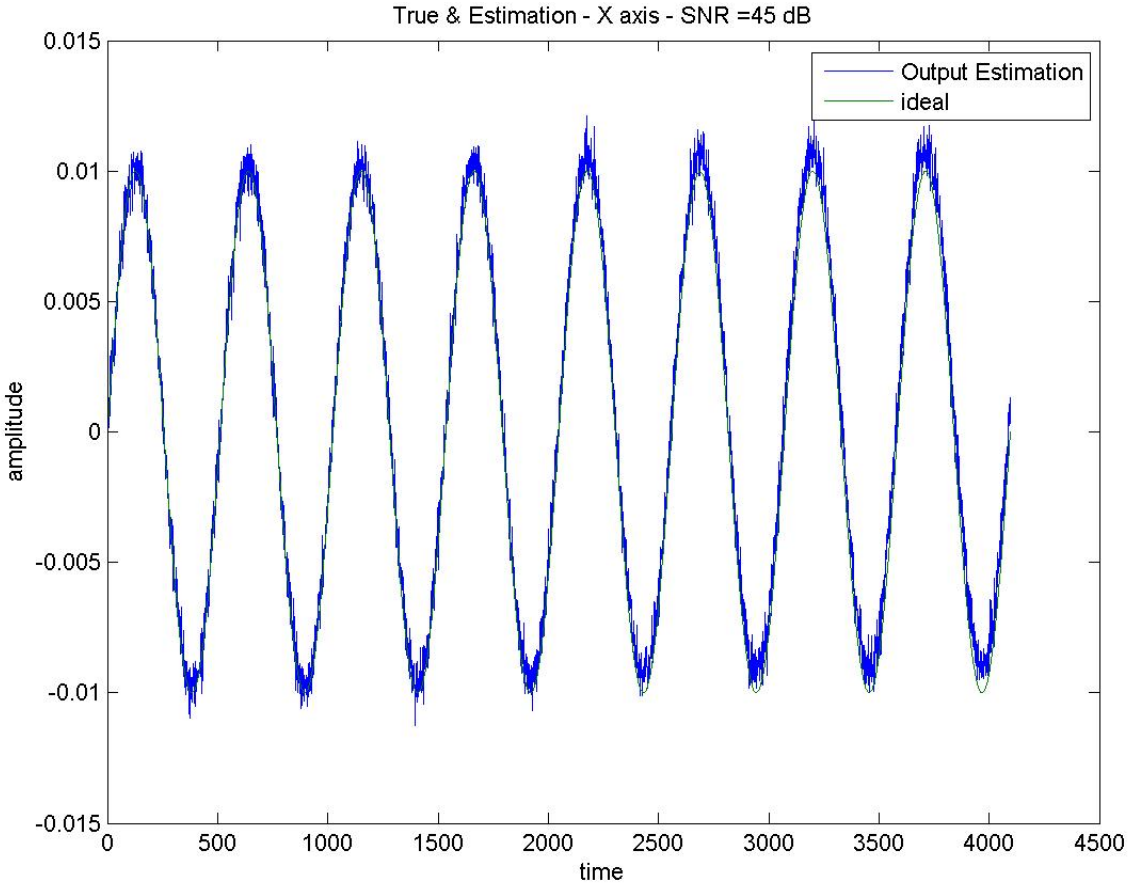

Figure 25: Estimated and true gravity along the z-axis at 45dB SNR for Model 2

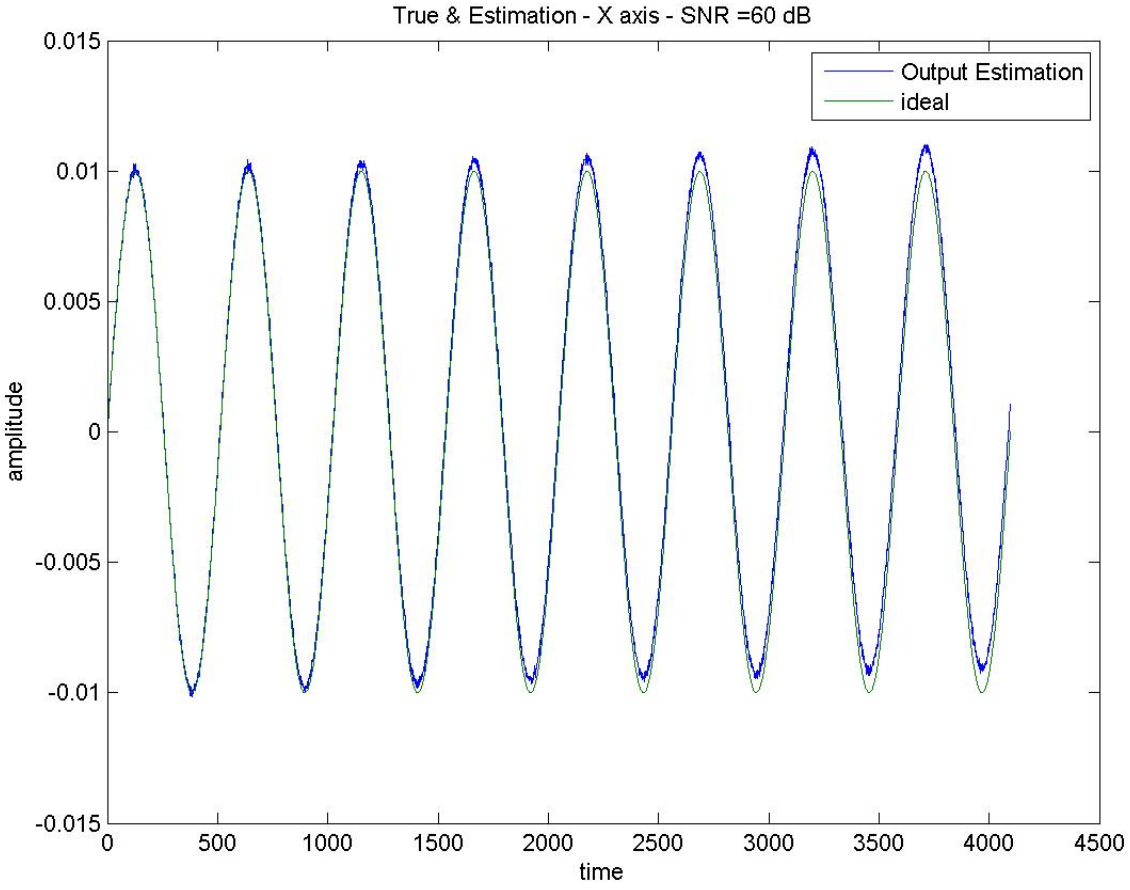

Figure 26: Estimated and true gravity along the z-axis at 60dB SNR for Model 2

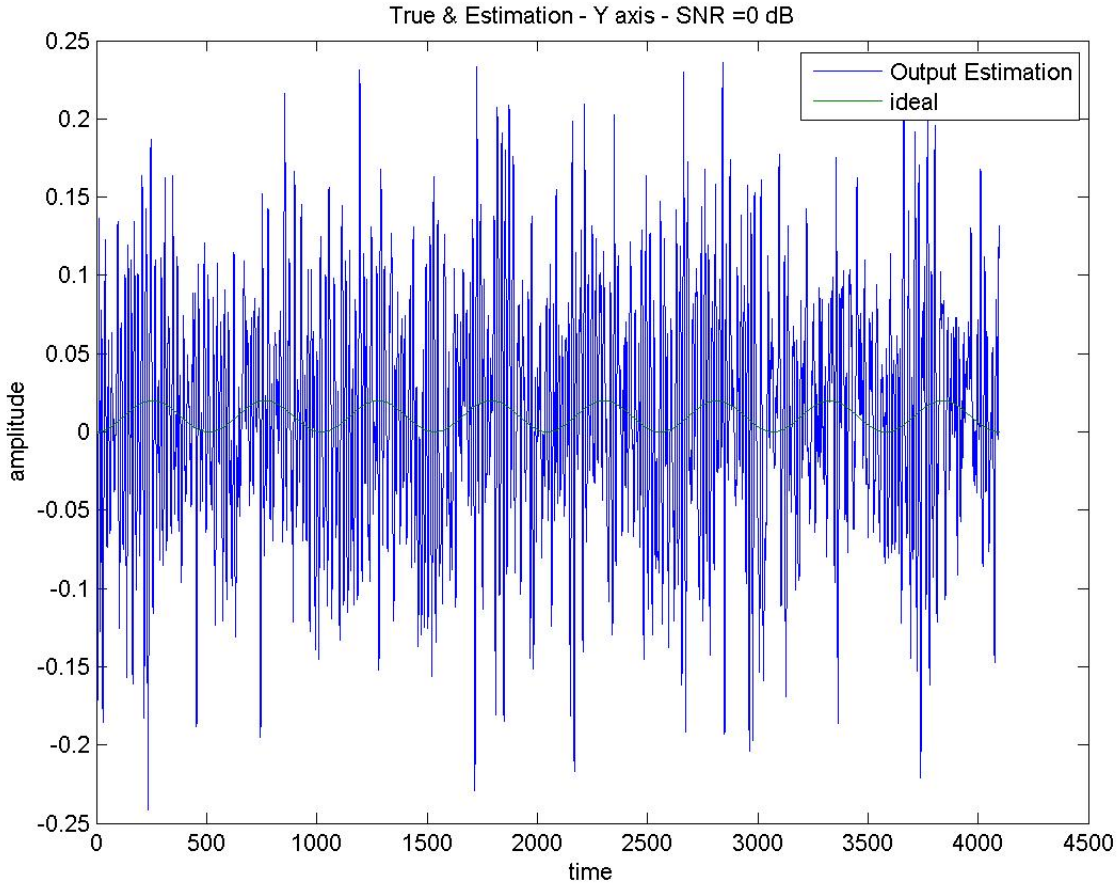

Figure 27: Estimation and true acceleration along the Y axis at 0dB SNR for Model 2

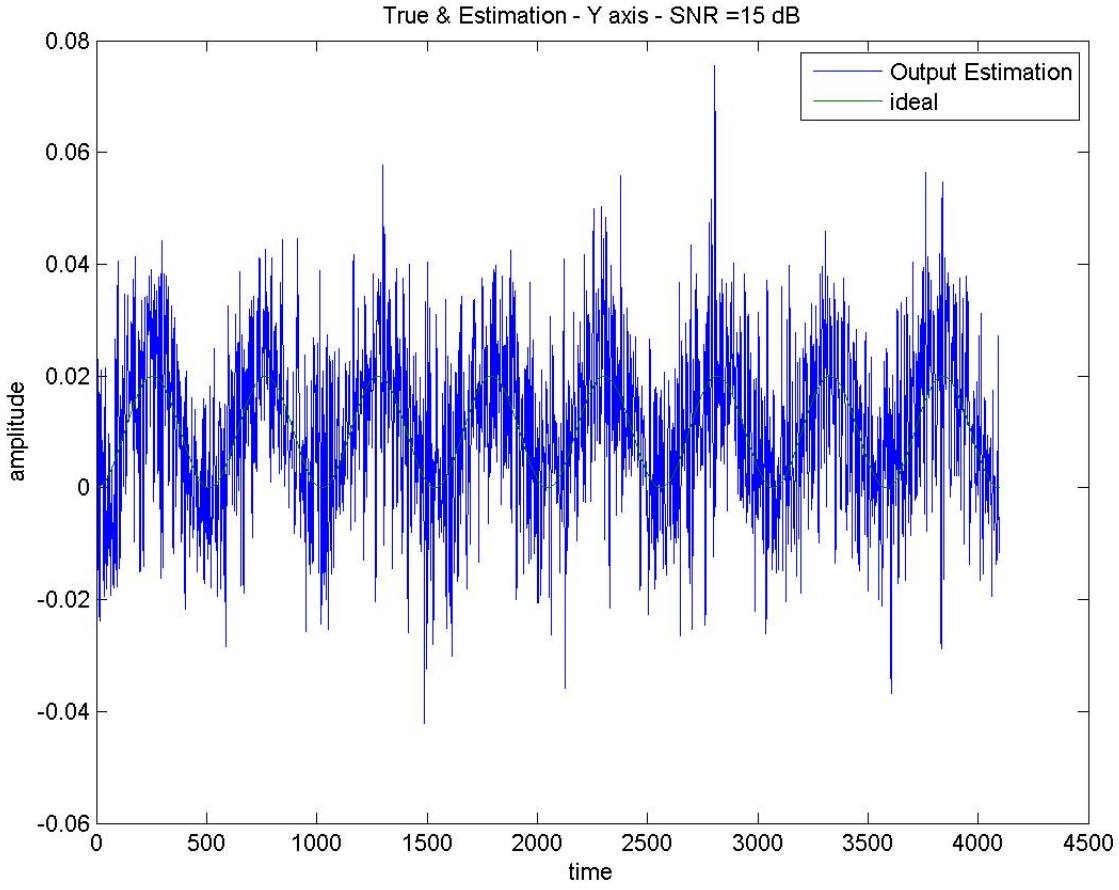

Figure 28: Estimation and true acceleration along the Y axis at 15dB SNR for Model 2

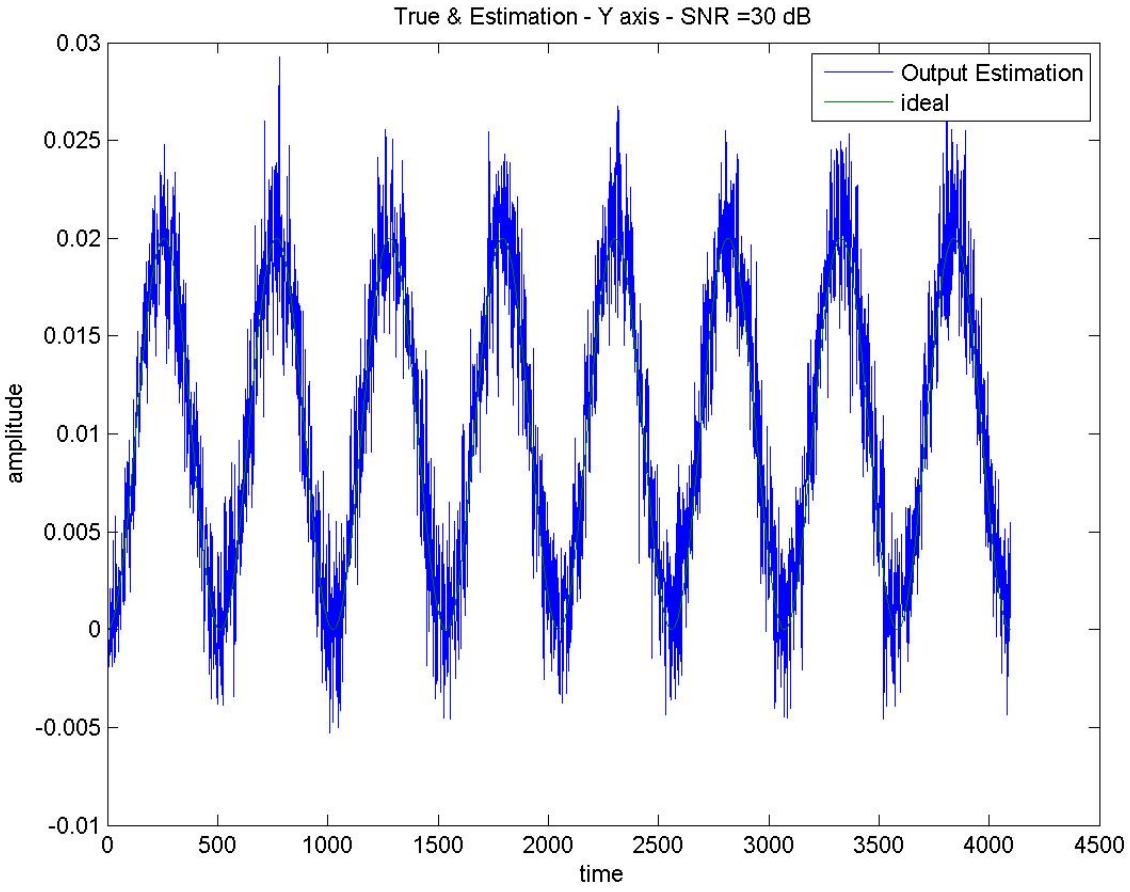

Figure 29: Estimation and true acceleration along the Y axis at 30dB SNR for Model 2

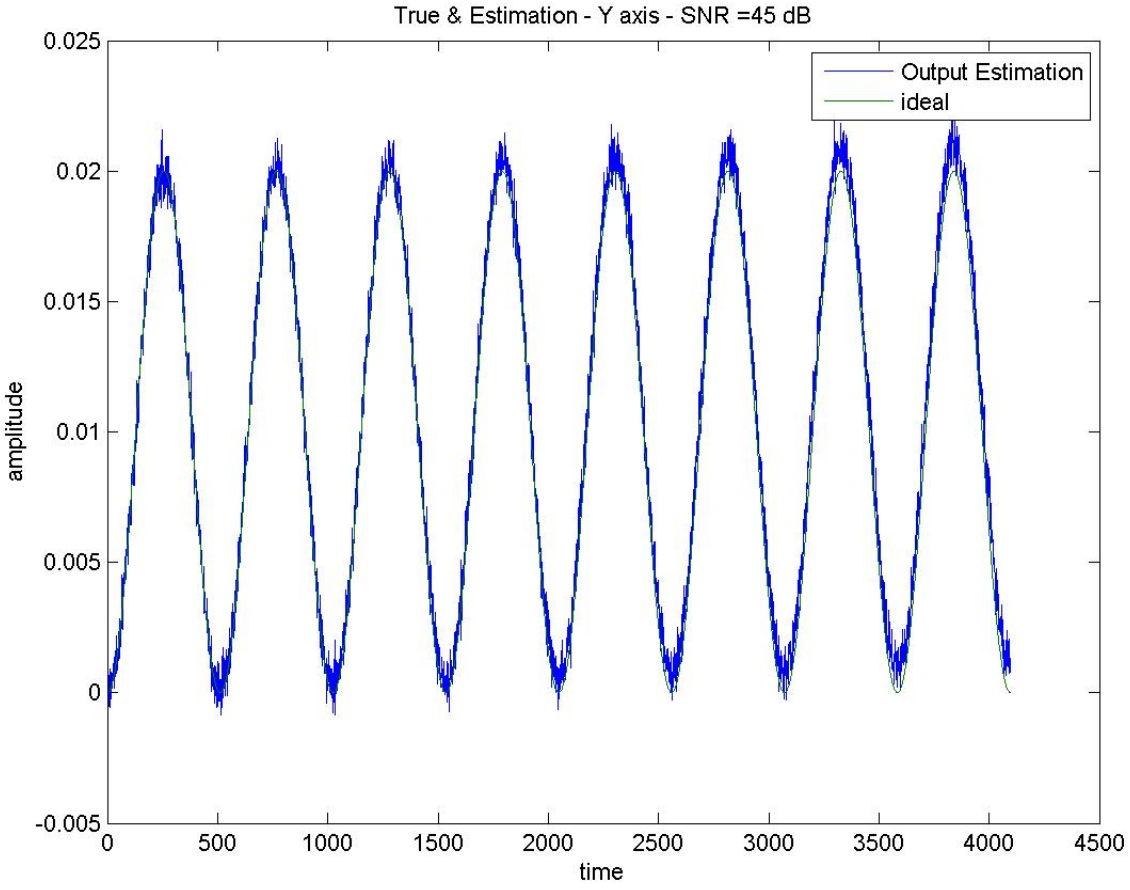

Figure 30: Estimation and true acceleration along the Y axis at 45dB SNR for Model 2

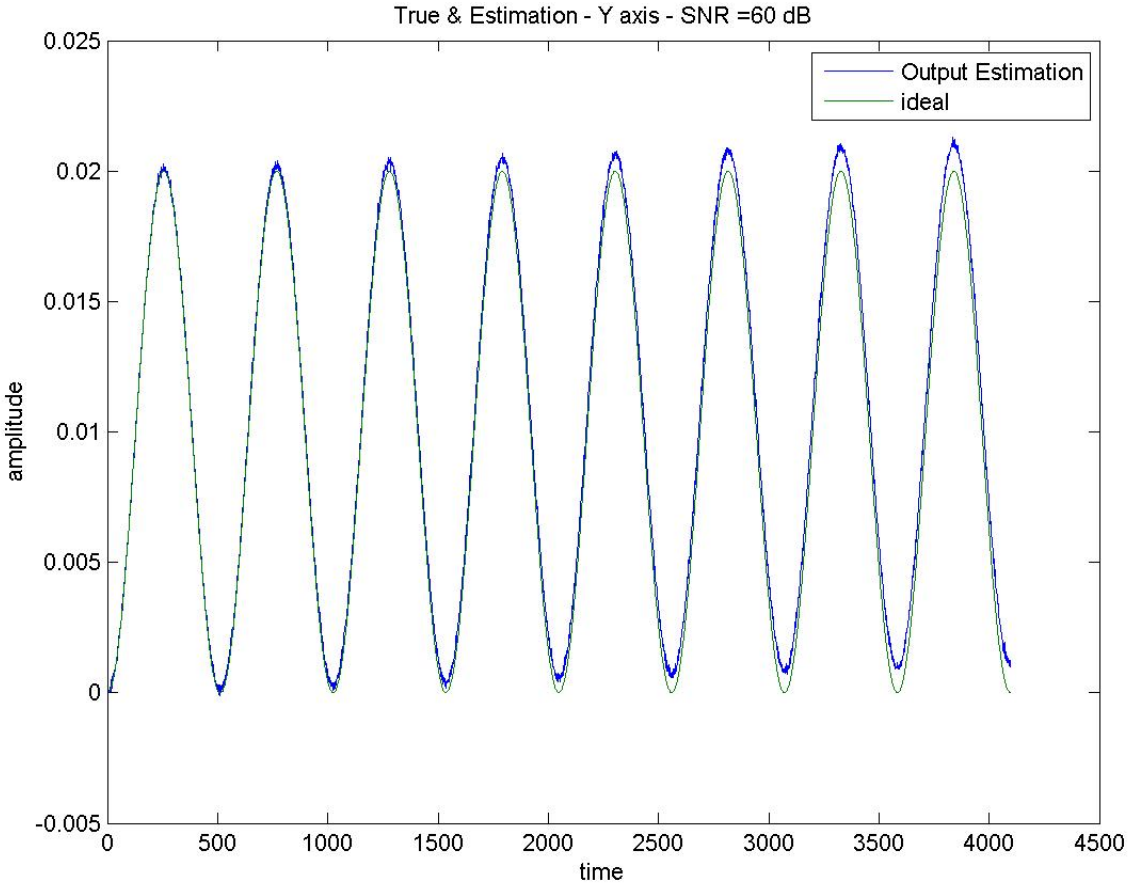

Figure 31: Estimation and true acceleration along the Y axis at 60dB SNR for Model 2

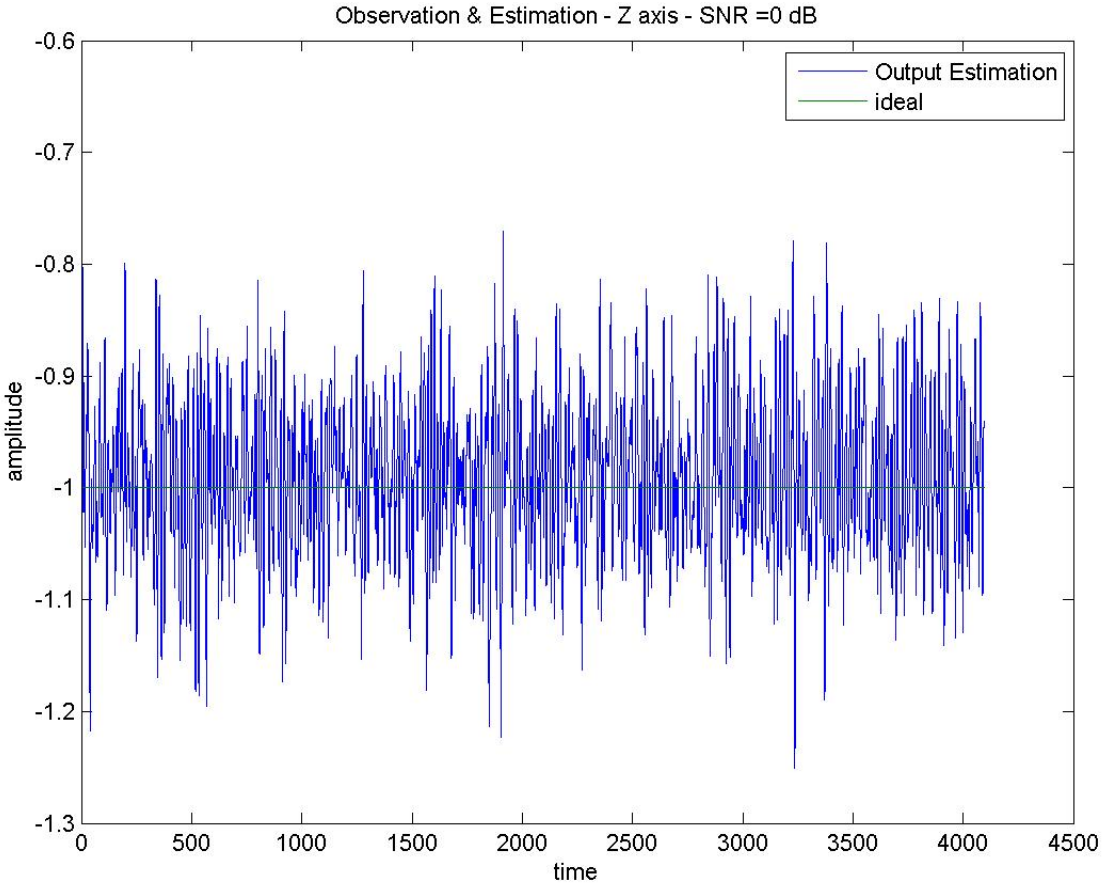

Figure 32: Estimation and true acceleration along the Z axis at 0dB SNR for Model 2

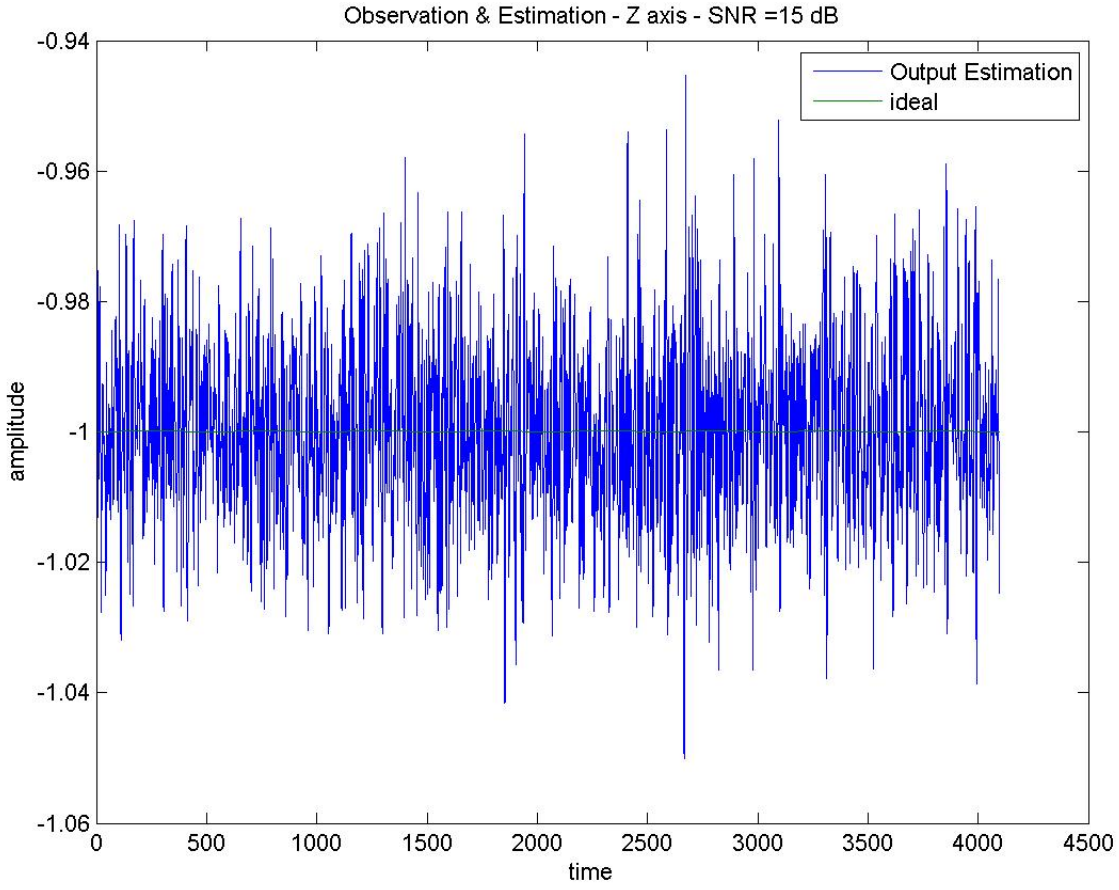

Figure 33: Estimation and true acceleration along the Z axis at 15dB SNR for Model 2

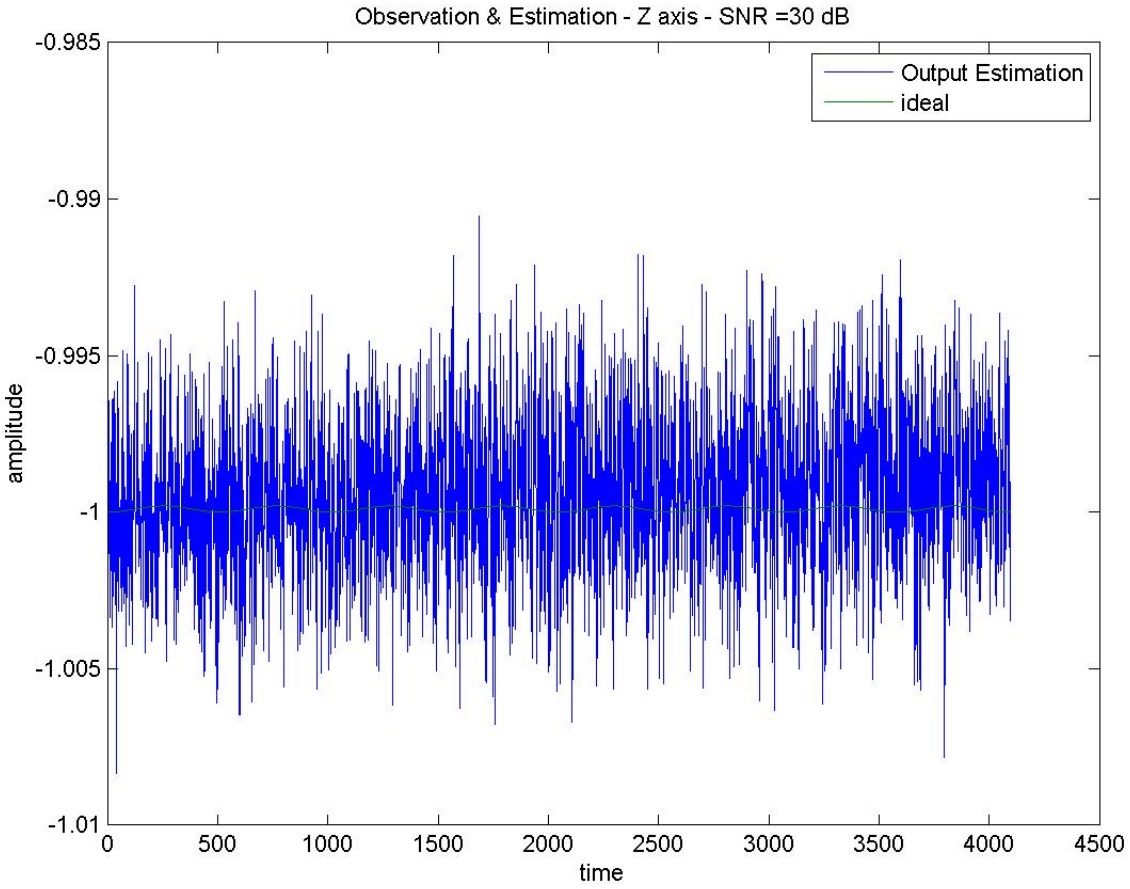

Figure 34: Estimation and true acceleration along the Z axis at 30dB SNR for Model 2

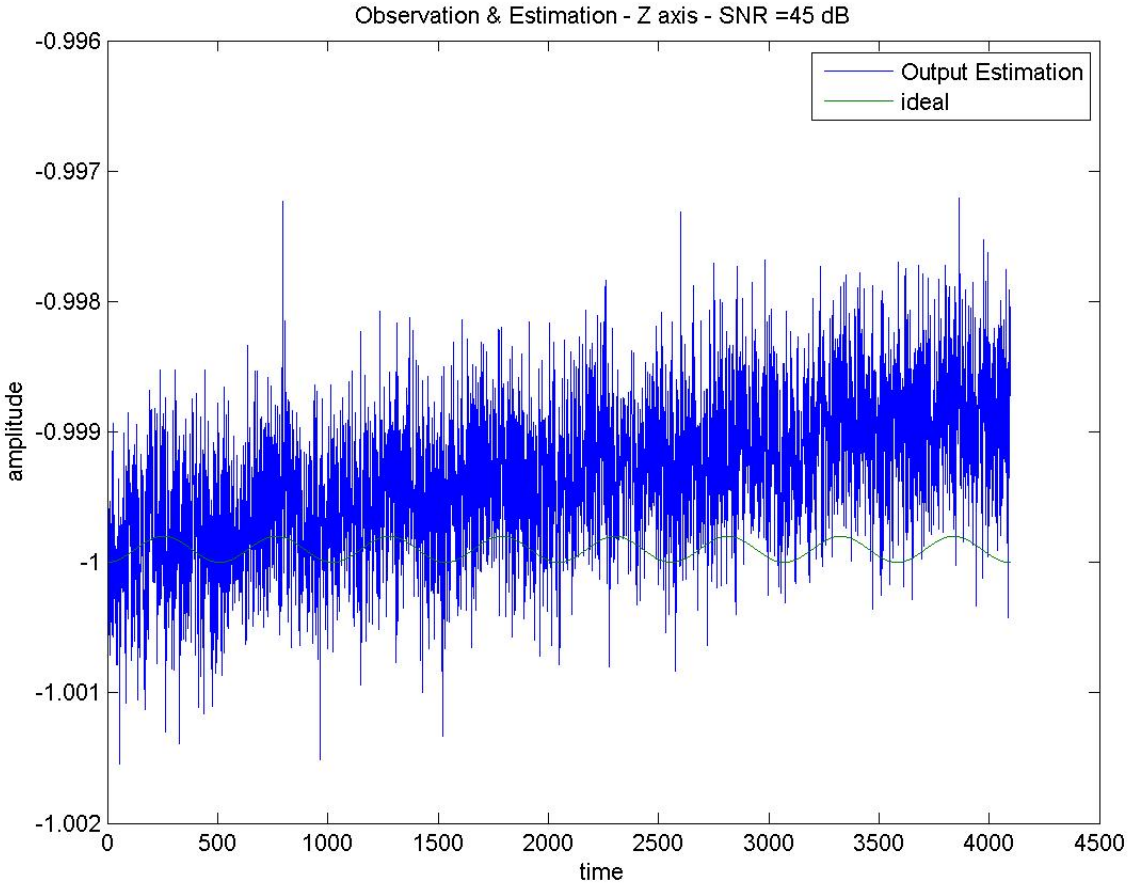

Figure 35: Estimation and true acceleration along the Z axis at 45dB SNR for Model 2

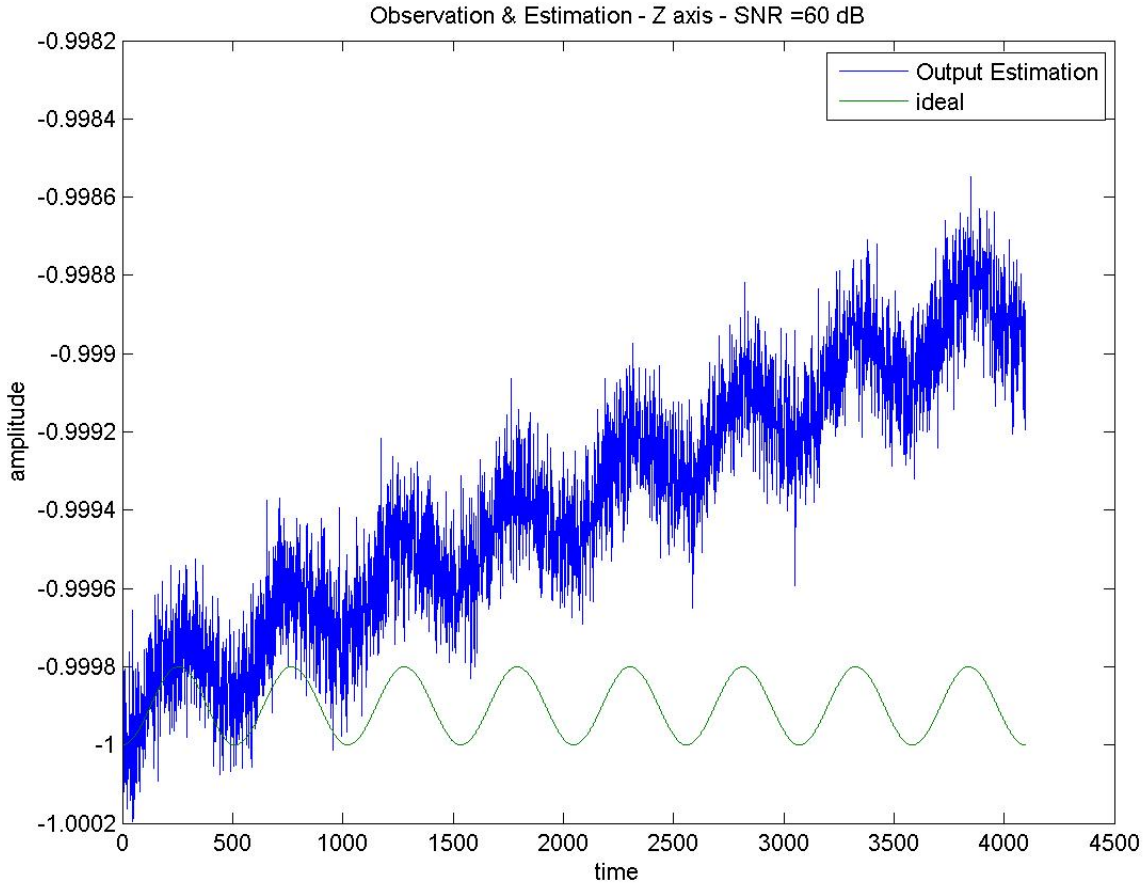

Figure 36: Estimation and true acceleration along the Z axis at 60dB SNR for Model 2

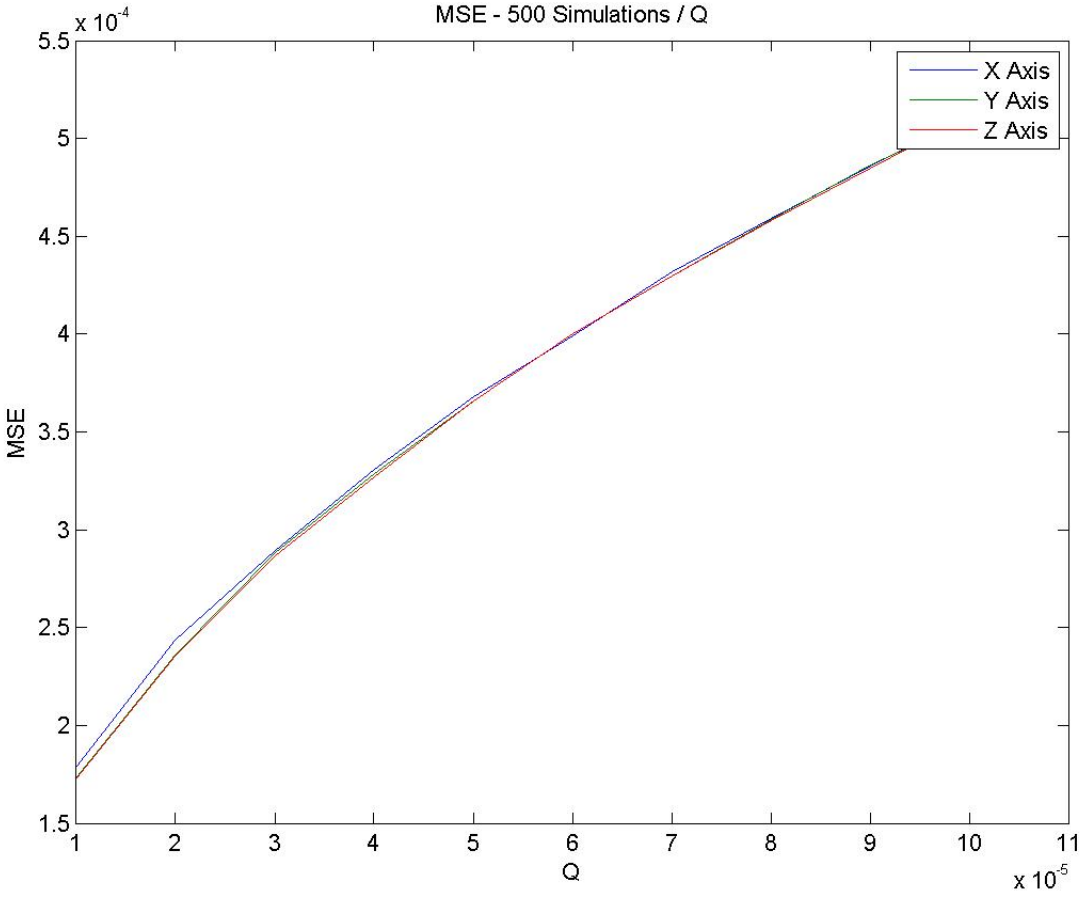

Figure 37: MSE Monte Carlo Results of Varying Q - Linear Scale

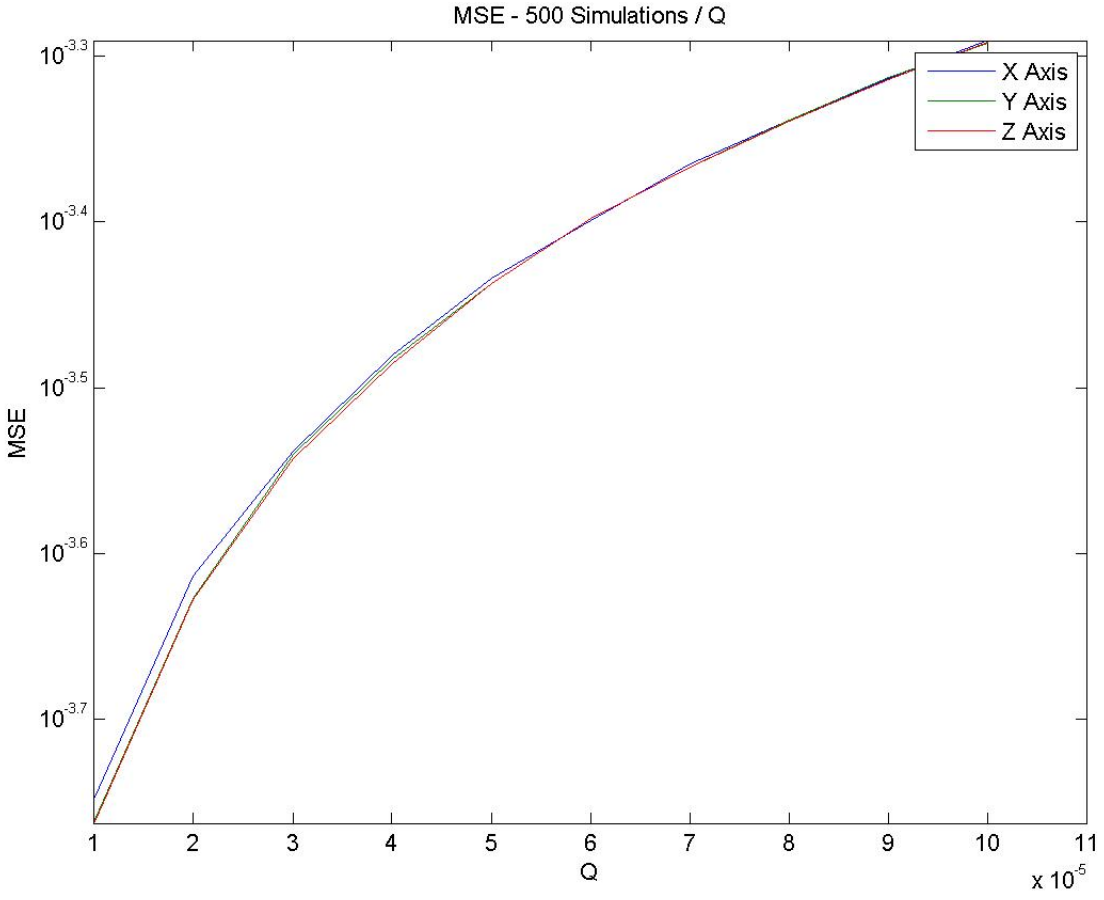

Figure 38: MSE Monte Carlo Results of Varying Q - Log Scale

Additionally, we did Monte Carlo simulations over 13 SNR values, ranging from 5 dB to 60 dB for each model. The Monte Carlo simulations were repeated 500 times for each SNR. We averaged over all time steps for each SNR. The resulting Mean Square Error (MSE) performance is shown in Figures 39, 40, 41, and 42. As expected, the MSE improves with SNR. Another observation is that Model 1 was a better estimator than Model 2 for low SNRs, but both converged as the SNR approached 60 dB. This fact was attributed to the nature of the signal at low SNR values because the true gravity model is very nonlinear and cannot not be estimated with a linear model. Model 2 assumes that the state increaes linearly with time and computes x_k by letting the state at time $k-1$ be the average of the state at time k and at time $k-2$ whereas Model 1 keeps the state the same upto some modeling error. By using the linearly increasing state assumption, we were introducing more errors than merely assuming the next estimate equated the current estimate.

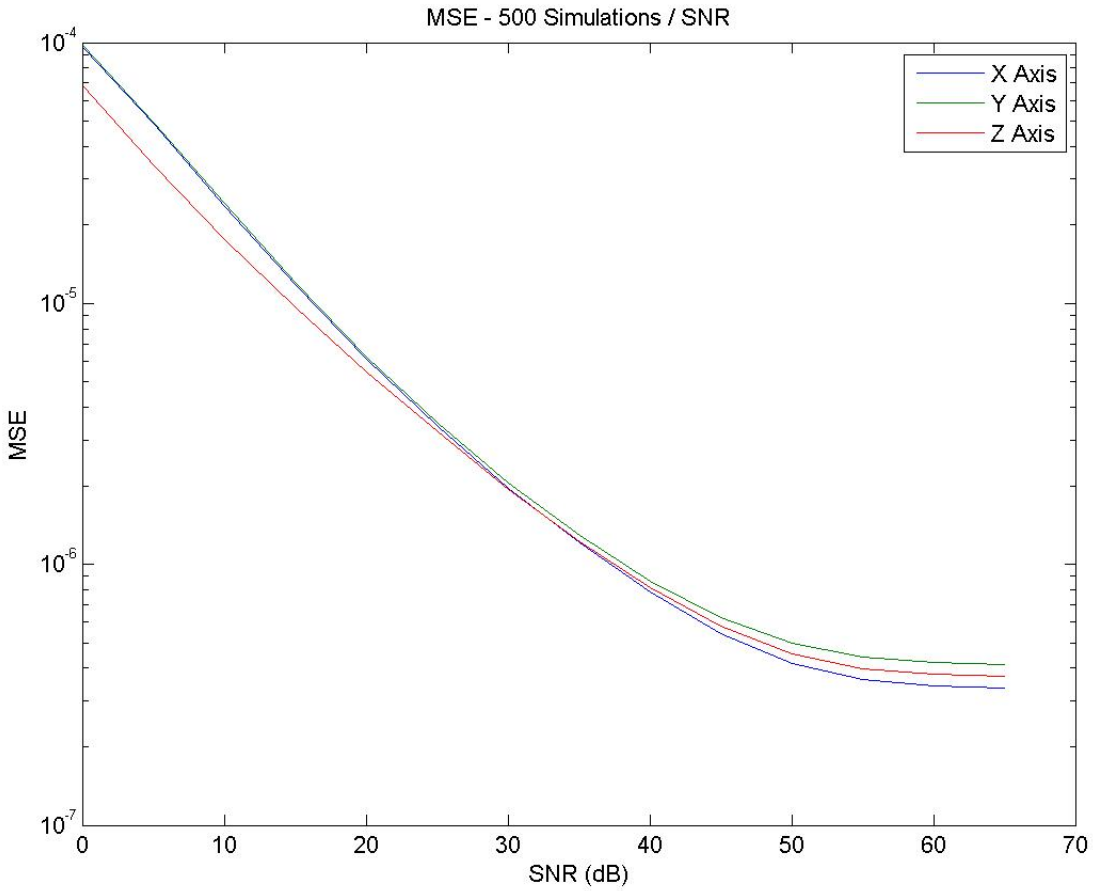

Figure 39: Averaged MSE of gravity estimates (x, y, and z components) for Model 1 with log scale

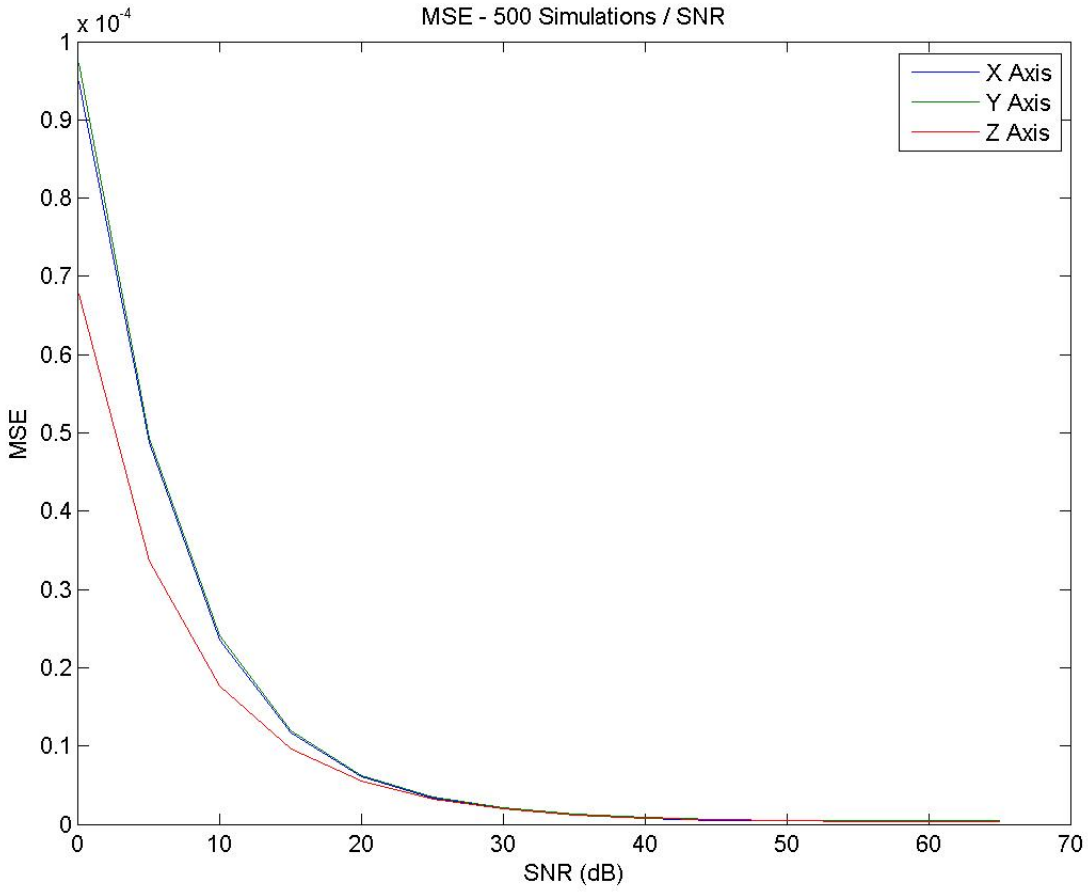

Figure 40: Averaged MSE of gravity estimates (x, y, and z components) for Model 1 with linear scale

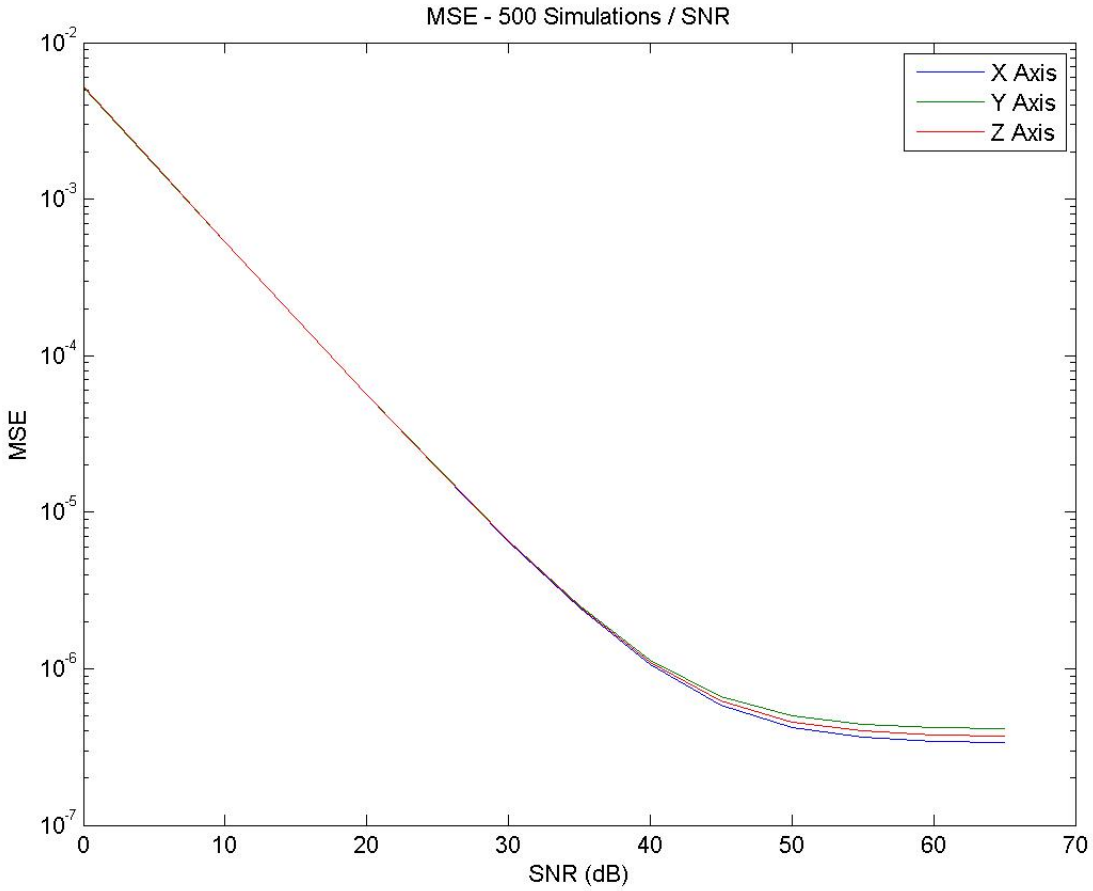

Figure 41: Averaged MSE of gravity estimates (x, y, and z components) for Model 2 with log scale

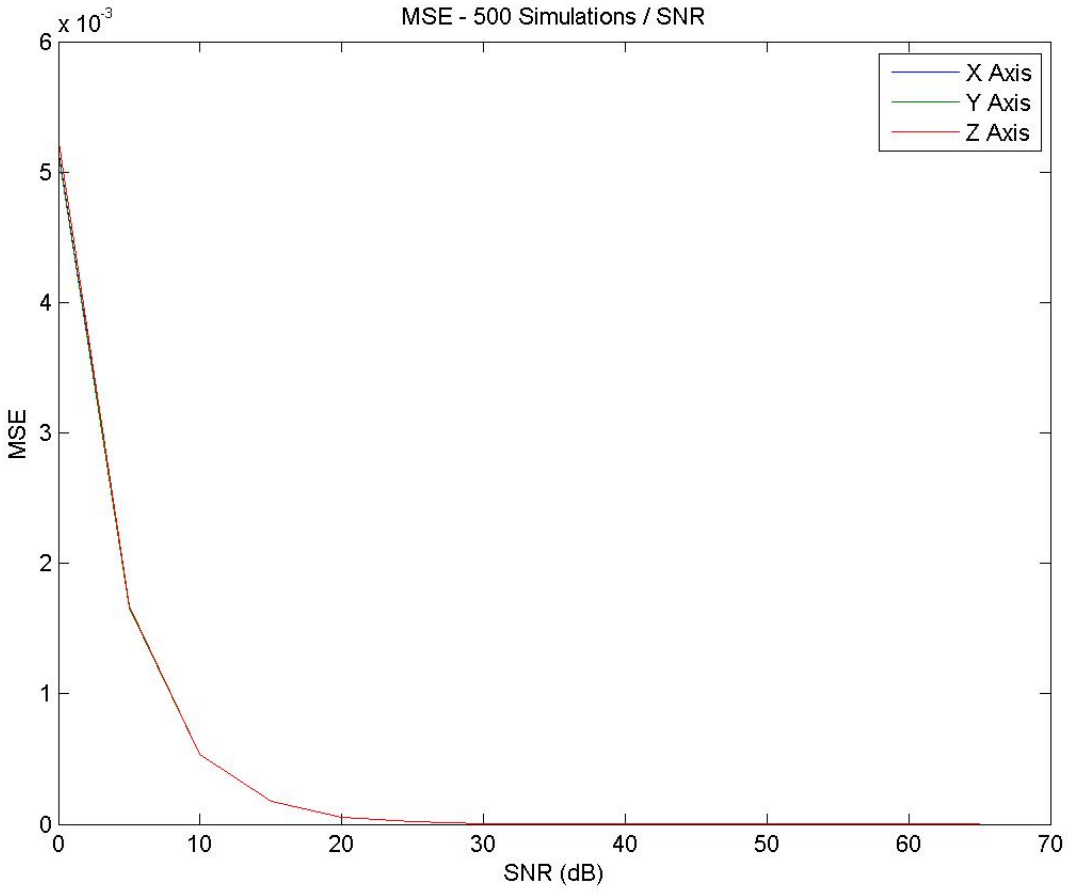

Figure 42: Averaged MSE of gravity estimates (x, y, and z components) for Model 2 with linear scale

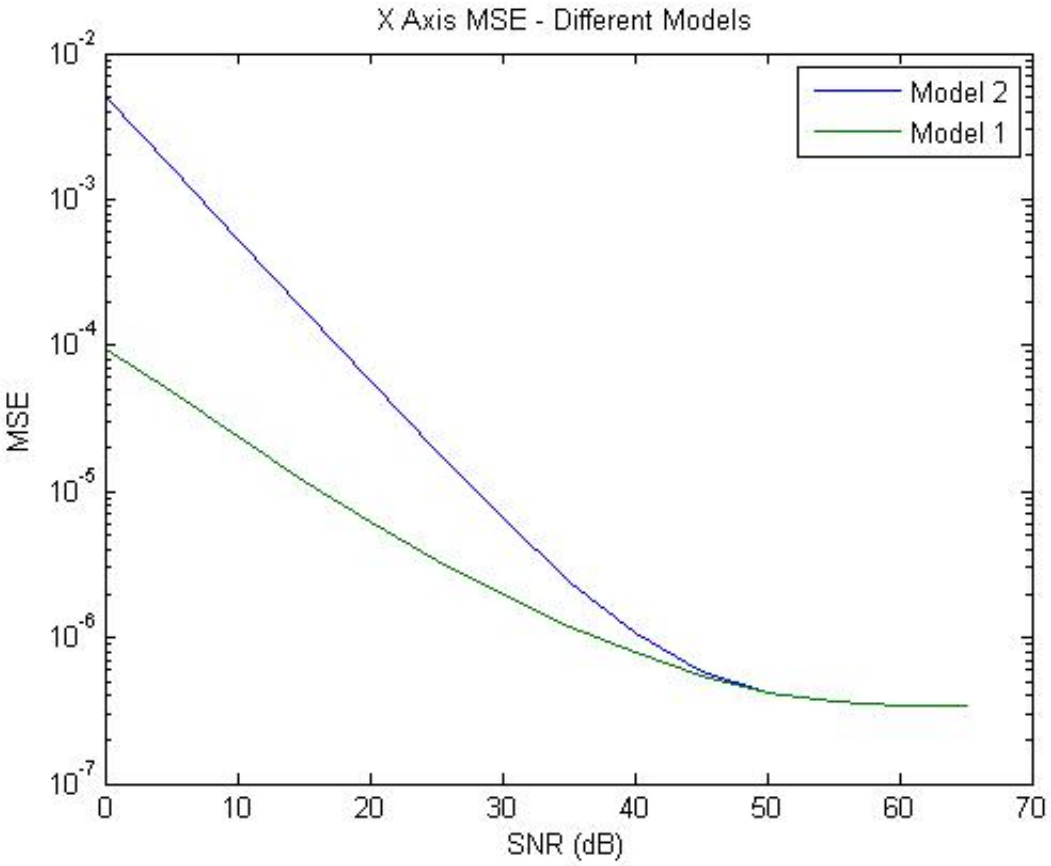

Figure 43: MSE of X Channel over 5dB to 60dB for both models

5 Conclusion

There is a significant amount of research in the area of human motion detection, estimation, classification, and quantification. As stated previously, most research falls into two groups, biologically advanced but signal processing deprived, and advanced signal processing but biologically deprived. The research outlined in this manuscript demonstrates the ability to provide both an advanced signal processing system that is biologically advanced as well as to produce new and innovative results for both the medical and engineering community. In the next few years, we will see a bridging of these areas as semiconductor technologies allow extremely low power electronics with complex mathematics to take place in an implanted or halter type device. Advanced methods like the Kalman filter, Particle Filtering, and other nonlinear estimation techniques will find themselves in biological applications in the very near future. As time goes on, we will discover just how much information we throw away for the sake of reduced power consumption. As we discover this, we will see broad jumps in medical diagnostic and therapy delivering devices.

5.1 Future Work

We plan to investigate four areas of accuracy improvement over the current model. The first area is to increase the accuracy of the physics equations. Currently, we do not take into account physics concepts. Our plan is to model gravity as well as the accelerations derived from human motion to improve model accuracy, and therefore performance. The next area is to increase the depth of the particle filter. Currently, we use only one historical data point to estimate the next point. If we extend that to use n points, we will see an improved accuracy, especially, if we use equations derived from more accurate physics. The third area is to determine the linearity of the system. If the system is too nonlinear (beyond being able to estimate it as linear), we will use particle fiiltering instead of Kalman filtering in order to improve the MSE performance. The fourth area is to examine the noise experienced in the

system. If the noise has a non-Gaussian distrobution, we will need to use a particle filter to properly process it. Once we have examined these areas, we plan on implementing this in synthesizable digital logic as an implantable biomedical signal processing unit. These new developments require looking into other forms of processing such as particle filters which tolerate non-Gaussian noise sources and nonlinear models.

References

[1] H. J. Luinge and P. H. Veltink, "Inclination measurement of human movement using a 3-D accelerometer with autocalibration," *IEEE Transactions on Neural Systems and Rehabilitation Engineering*, pp. 112–121, 2004.

[2] N. Noury, P. Barralon, P. Couturier, F. Favre-Rguillon, R. Guillemaud, C. Mestais, Y. Caritu, D. David, S. Moine, A. Franco, F. Guiraud-By, M. Brenguer, and H. Provost, "A MEMS based microsystem for the monitoring of the activity of frail elderly in their daily life: The actidom project," in *6th International Workshop on Enterprise Networking and Computing in Healthcare Industry, 2004.*, pp. 105–109, 2004.

[3] A. Wixted, D. Thiel, D. James, A. Hahn, C. Gore, and D. Pyne, "Signal processing for estimating energy expenditure of elite athletes using triaxial accelerometers," *Sensors*, pp. 798–801, 2005.

[4] R. Zhu and Z. Zhou, "A real-time articulated human motion tracking using tri-axis inertial/magnetic sensors package," *IEEE Transactions on Neural Systems and Rehabilitation Engineering*, pp. 295–302, 2004.

[5] J. Lan, T. Lan, and S. Nahavandi, "A novel application of a microaccelerometer for target classification," *IEEE Sensors Journal*, pp. 319–324, 2004.

[6] M. A. D. Raya and L. G. Sison, "Adaptive noise canceling of motion artifact in stress ecg signals using accelerometer," in *Proceedings of the Second Joint EMBS/BMES Conference*, pp. 1756–1757, 2002.

[7] P. H. Veltink and H. M. Franken, "Detection of knee unlock during stance by accelerometry," *IEEE Transactions on Rehabilitation Engineering*, pp. 395–402, 1996.

[8] S. H. Nawab, S. H. Roy, and C. J. D. Luca, "Functional activity monitoring from wearable sensor data," in *Proceedings of the 26th Annual International Conference of the IEEE EMBS*, pp. 979–982, 2004.

[9] I. J. Jang and W. B. Park, "Signal processing of the accelerometer for gesture awareness on handheld devices," in *Proceedings of the 2003 IEEE International Workshop on Robot and Human Interactive Communication*, pp. 139–144, 2003.

[10] T. Wark and M. Karunanithi, "A framework for linking gait characteristics of patients with accelerations of the waist," in *Proceedings of the 2005 IEEE Engineering in Medicine and Biology 27th Annual Conference*, pp. 7695–7698, 2005.

[11] H. Dejnabadi, B. M. Jolles, and K. Aminian, "A new approach to accurate measurement of uniaxial joint angles based on a combination of accelerometers and gyroscopes," *IEEE Transactions on Biomedical Engineering*, pp. 1478–1484, 2005.

[12] S. Tanaka, K. Motoi, M. Nogawa, and K. Yamakoshi, "A new portable device for ambulatory monitoring of human posture and walking velocity using miniature accelerometers and gyroscope," in *Proceedings of the 26th Annual International Conference of the IEEE EMBS*, pp. 2283–2286, 2004.

[13] B. Najafi, K. Aminian, A. Paraschiv-Ionescu, F. Loew, C. J. Bula, and P. Robert, "Ambulatory system for human motion analysis using a kinematic sensor: Monitoring of daily physical activity in the elderly," *IEEE Transactions on Biomedical Engineering*, pp. 711–723, 2003.

[14] L. Hoff, O. Elle, M. Grimnes, S. Halvorsen, H. Alker, and E. Fosse, "Measurements of heart motion using accelerometers," in *Proceedings of the 26th Annual International Conference of the IEEE EMBS*, pp. 2049–2051, 2004.

[15] M. Naing, F. E. Hock, T. Hong, Y. Yiow, and K. Luck, "Location and sensitivity comparison of MEMS accelerometers in signal identification for ambulatory monitoring," in *2004 Electronic Components and Technology Conference*, pp. 956–960, 2004.

[16] J. Mantyjarvi, M. Lindholm, E. Vildjiounaite, S.-M. Makela, and H. Ailisto, "Identifying users of portable devices from gait pattern with accelerometers," in *ICASSP*, pp. 973–976, 2005.

[17] H. J. Luinge, P. Veltink, and C. Baten, "Estimation of orientation with gyroscopes and accelerometers," in *First Joint BMES/EMBS Conference Serving Humanity, Advancing Technology*, p. 844, 1999.

[18] K. Motoi, S. Tanaka, M. Nogawa, and K. Yamakoshi, "Evaluation of a new sensor system for ambulatory monitoring of human posture and walking speed using accelerometers and gyroscope," in *SICE Annual Conference in Fukui*, pp. 1232–1235, 2003.

[19] J. Y. Hwang, J. M. Kang, Y. W. Jang, and H. C. Kim, "Development of novel algorithm and real-time monitoring ambulatory system using bluetooth module for fall detection in the elderly," in *26th Annual International Conference of the IEEE EMBS*, pp. 2204–2207, 2004.

[20] M. Makikawa and D. Murakami, "Development of an ambulatory physical activity and behavior map monitoring system," in *18th Annual International Conference of the IEEE Engineering in Medicine and Biology Society*, pp. 71–72, 1996.

[21] D. Cooper, "Comparison of activity sensors and algorithms for rate-responsive pacemakers using ambulatory monitoring," *IEEE Computers in Cardiology*, pp. 851–854, 1993.

[22] D. Roetenberg, P. Slycke, and P. H. Veltink, "Ambulatory position and orientation tracking fusing magnetic and inertial sensing," *IEEE Transactions of Biomedical Engineering*, pp. 1–8, 2006.

[23] I. Kobayashi, A. Sugawara, R. Hayashi, and H. Matsumoto, "Telemetry system of daily life motion and arrythmia," in *Proceedings - 19th International Conference - IEEE/EMBS*, pp. 2229–2231, 1997.

[24] A. Wixted, D. Theil, A. Hahn, C. Gore, D. Pyne, and D. James, "Measurement of energy expenditure in elite athletes using MEMS-based triaxial accelerometers," *IEEE Sensors Journal*, pp. 481–488, 2007.

[25] D. James, N. Davey, and T. Rice, "An accelerometer based sensor platform for insitu elite athlete performance analysis," *Proceedings of IEEE Sensors*, pp. 1373–1376, 2004.

[26] F. Allen, E. Ambikairajah, N. Lovell, and B. Celler, "An adapted gaussian mixture model approach to accelerometry-based movement classification using time-domain features," in *Proceddings of the 28th IEEE EMBS Annual International Conference*, pp. 3600–3603, 2006.

[27] M. Sekine, Y. Abe, M. Sekimoto, Y. Higashi, T. Fujimoto, T. Tamura, and Y. Fukui, "Assessment of gait parameter in hemiplegic patients by accelerometry," in *Proceedings of the 22nd Annual EMBS International Conference*, pp. 1879–1882, 2000.

[28] D. Karantonis, M. Narayanan, M. Mathie, N. Lovell, and B. Celler, "Implementation of a real-time human movement classifier using a triaxial accelerometer for ambulatory monitoring," *IEEE Transactions on Information Technology in Biomedicine*, pp. 156–167, 2006.

[29] "Wikipedia - kalman filter," 2008.

[30] "Wikipedia - particle filter," 2008.